Identification of a novel type of glucose dehydrogenase involved in the mineral weathering ability of Collimonas pratensis strain PMB3(1)

Laura Picard, Marie-Pierre M.-P. Turpault, P. Oger, Stephane Uroz

TITLE: Identification of a novel type of glucose dehydrogenase involved in the mineral weathering ability of *Collimonas pratensis* strain PMB3(1)

Running title: Mineral weathering by a glucose dehydrogenase

AUTHORS: Picard, L.[1,2], Turpault, M-P. [2], Oger, P.M.[3], Uroz, S. [1,2#]

[1] Université de Lorraine, INRAE, UMR1136 « Interactions Arbres-Microorganismes », F-54280 Champenoux, France

[2] INRAE, UR1138 « Biogéochimie des écosystèmes forestiers », F-54280 Champenoux, France

[3] Université de Lyon, INSA de Lyon, CNRS UMR 5240, Lyon, France

 # Corresponding author: Mailing address:
Université de Lorraine, INRAE, "Interactions Arbres Microorganismes", UMR 1136, 54280 Champenoux, France. Phone: +33 (0)3 83 39 40 81, Fax: +33 (0)3 83 39 40 69. E-mail: stephane.uroz@inra.fr.

Key words: *Collimonas pratensis* PMB3(1), mineral weathering, Glucose/Methanol/Choline oxidoreductase, PQQ-independent glucose dehydrogenase, biotite

ABSTRACT

The exact molecular mechanisms as well as the genes involved in the mineral weathering (MW) process by bacteria remain poorly characterized. To date, a single type of glucose dehydrogenase (GDH) depending on a particular co-factor named pyrroloquinoline quinone (PQQ) is known. These enzymes allow the production of gluconic acid through the oxidation of glucose. However, it remains to be determined how bacteria missing PQQ-dependent GDH and/or the related *pqq* biogenesis genes weather minerals. In this study, we considered the very effective mineral weathering bacterial strain PMB3(1) of *Collimonas pratensis*. Genome analysis revealed that it does not possess the PQQ based system. The use of random mutagenesis, gene complementation and functional assays allowed us to identify mutants impacted in their ability to weather mineral. Among them, three mutants were strongly altered on their acidification and biotite weathering abilities (58 to 75% of reduction compared to WT) and did not produce gluconic acid. The characterization of the genomic regions allowed noticeably to the identification of a Glucose/Methanol/Choline oxidoreductase. This region appeared very conserved among collimonads and related genera. This study represents the first demonstration of the implication of a PQQ-independent GDH in the mineral weathering process and explains how *Collimonas* weather minerals.

INTRODUCTION

Minerals represent physical supports and reservoirs of nutritive elements for the development of the biosphere. Their dissolution, *i.e*., mineral weathering (MW), participates in the release of their nutritive constituents. This essential process permits to maintain the relative fertility of the soils and to support the growth of the plants. In nutrient-poor and non-amended environments such as forests, minerals are considered as one of the most important stock of nutrients for the long-lasting development of the ecosystem (Ranger and Turpault, 1999). However, MW is a slow process, which depends on the intrinsic properties of those minerals (*i.e.*, dissolution constant) and extrinsic conditions that result from a combination of abiotic and biotic processes. For instance, in acidic draining medium, biotite dissolves faster than quartz because of their intrinsic properties (*i.e*., chemical composition) (Brantley, 2008). In drained soils, water and acid circulation are known as important abiotic factors involved in the dissolution of minerals. Plants and soil microorganisms are also known to participate in this process (Gadd, 2007; Landeweer*t et a*l. 2001). Tree roots and fungal hyphae can physically weather minerals (*i.e*., division) through the pressure applied (Bonneville *et a*l. 2009). Plant development through nutrient pumping and rhizosphere acidification induces stronger MW than in the surrounding bulk soil (Calvaruso et al. 2009; Turpault et al. 2009; Hinsinger et al. 2003). The production of chelating and acidifying agents was also reported for a wide range of plants, symbiotic fungi and bacteria (Jongman*s et al*. 1997; Uro*z et a*l. 2009a).

Effective MW bacteria have been described in various environments, and especially in the rhizosphere of different plants (*i.e*., trees, cactus) living in nutrient-poor environments (Puente et al. 2004). Notably, several studies evidenced a significant enrichment of these functional communities in the rhizosphere compared to the surrounding bulk soil (Collignon*et a*l. 2011; Calvarus*o et al*. 2010; Zhang *et* al. 2016). In addition, microcosm experiments revealed that

effective MW bacterial strains can improve plant growth. Indeed, the inoculation or co-inoculation of different MW bacterial strains was shown to increase the seedling biomass, the shoot length, the root biomass, the total root length and the total root surface area of *Pinus sylvestris* compared to non-inoculated plants (Calvarus*o et al*. 2006; Koel*e et a*l. 2009). To date, the ability to solubilize mineral has been reported for a wide range of bacterial genera (*i.e*., *Achromobacter, Agrobacterium, Bacillus, Collimonas, Pseudomonas, Rhizobium, Burkholderia, Microccocus, Aereobacter, Flavobacterium* or *Erwinia*) (Puent*e et a*l. 2004; , Collignon *et al*. 2011; Rodriguez and Fraga, 1999; Uroz *et a*l. 2011).

If the ability of the bacteria to weather minerals is well documented, our understanding of the molecular basis and especially of the genes involved in MW remains limited. This gap of knowledge has seriously hampered studies of the ecology, evolution and relative role of the mineral weathering bacteria. To date, no molecular tools exist to assess and quantify the occurrence, diversity, and activity of mineral weathering genes in natural bacterial populations. Heterotrophic bacteria are known to produce chelating agents (*i.e*., siderophores and organic acids) and acidifying metabolites (*i.e*., protons, organic acids), but the molecular demonstrations of their relative role in the MW process are limited as well as is our knowledge of the conservation among bacteria of the molecular markers involved. Considering the organic acid production, several studies showed that the direct oxidation pathway of glucose is involved and more specifically the steps producing gluconic acid (GA) and 2-ketogluconic acid (2KGA) through the activity of a glucose dehydrogenase (GDH) and a gluconate dehydrogenase (GADH), respectively (Goldstein, 1995). To date, the demonstration of the link between phosphate dissolution and the activity of the GDH activity was obtained on a wide range of bacterial genera. All these studies highlighted the implication of a specific type of GDH that depends on a particular cofactor, the pyrroloquinoline quinone (PQQ) (Goldstein *et al*. 2003; Babu-Kha*n et a*l. 1995; Li*u et al*. 1992; Wag*h et a*l. 2014).

The implication of a PQQ-dependent GDH enzyme in the dissolution of a complex mineral, biotite, was recently evidenced for a strain of *Pseudomonas* (Wa*ng et a*l. 2020).

In this study, we investigated the molecular basis of MW in the model bacterial strain *Collimonas pratensis* PMB3(1), which was shown to be very effective at MW (Uro*z et* al. 2007; Uro*z et a*l. 2009a). This bacterial genus is usually considered as member of the rare biosphere due to its low representativeness in metagenomic data from soil (Levea*u et a*l. 2010). However, collimonads can represent dominant taxa in specific habitats such as on mineral particles or in the mycorrhizosphere (Lepleux *et al.* 2012; Uroz *et al*. 2012, Colin *et al*. 2017). Collimonads are recognized as particularly effective at mobilizing nutrients from recalcitrant sources such as chitin and minerals, suggesting that they are particularly well adapted to live in nutrient-poor conditions (Levea*u et a*l. 2010). Their strong MW effectiveness was suggested to be linked to their ability to acidify the medium in presence of glucose and to produce high amounts of gluconic acid (Uroz *et al.* 2009b). Using a random mutagenesis approach, associated to a functional screening and a gene complementation and chemical analyses, we identified the genes involved in the MW ability of strain PMB3(1) and evidenced a novel MW pathway involving a PQQ-independent, synthesis of gluconic acid, encoded by a glucose dehydrogenase (GDH).

MATERIALS AND METHODS

Bacterial strains and growth media. Bacterial strains and plasmids are listed in Table 1. The model bacterial strain *Collimonas pratensis* PMB3(1) considered in this study was isolated from oak (*Quercus petraea*)–*Scleroderma citrinum* ectomycorrhizae sampled in the organo-mineral soil horizon from the long term experimental forest site of Breuil-Chenue located in the Morvan region (France; for sampling details see Calvaruso et al. 2007). Strain PMB3(1)

was isolated from the symbiotic fungal mantle of the mycorrhizal fungus. Previous experiments showed that the strain PMB3(1) was particularly effective at weathering mineral (Uroz *et al.* 2007, 2009b). All strains were grown at 25°C, except the strains of *Escherichia coli*, which were grown at 37°C. The media used were Luria-Bertani (LB), AB medium (Chilton *et a*l. 1974) and a modified version of the Bushnell-Haas (BHm; devoid of iron) medium (Uroz *et a*l. 2007). The AB minimal (ABm) medium was supplemented with mannitol (2 g/l final concentration) as carbon source. The BHm medium was supplemented with glucose (2 g/l final concentration) as carbon source. Glucose was selected in our experiments because it represents the dominant carbohydrate source found in forest soil and in plant root exudates (Jolivet *et al*. 2006; Medeiros *et al*. 2006; Grayston and Campbell, 1996). Its presence is also explained by hydrolysis of various compounds such as starch, saccharose (Derrien *et al.* 2004) or by hydrolysis of trehalose, a carbohydrate accumulated in mycorrhizal roots (Martin *et al.* 1985). Antibiotics, when required, were added to the media at the following final concentrations: Tetracycline 10 µg/ml, Kanamycin 100 µg/ml and Ampicillin 100 µg/ml.

Tn5-OT182 mutagenesis. The wild-type strain PMB3(1) of *C. pratensis* was mutagenized with Tn5-OT182 as described previously (Deshazer *et a*l. 1997; Dennis *et a*l. 1998), with minor modifications. The donor strain, *E. coli* S17-1λpir (pOT182), was grown at 37°C in antibiotic-containing LB broth overnight, and the recipient strain, *C. pratensis* PMB3(1), was grown at 25°C in ABm liquid medium for 2 days. The day of the bi-parental conjugation, each culture (30 ml) was centrifuged and washed twice with sterile MQ water to remove any antibiotic from the medium and mixed in a final volume of 5 ml of sterile MQ water. The mixed suspension was spotted on agar LB plates (*i.e.*, 10 µl drops). After 5h of incubation at 25°C, the bacterial lawn of each plate was harvested using sterile MQ water (5 ml), and 150

µl of this suspension were plated on tetracycline-containing ABm plates for isolation of the Tn5 mutants of the strain PMB3(1). A total of 2,000 mutants able to grow on ABm supplemented with mannitol and tetracycline were recovered after 5 days incubation at 25°C and organized in 96-well microplates. To confirm the presence of the plasposon in the mutant genome, a portion of the plasposon sequence was amplified by PCR using pOT-For and pOT-Rev primers (Table 1). The quality of the mutant library was tested on a subset of Tn5 mutants and on the mutants of interest to determine whether the library was formed by independent events.

DNA manipulations and plasposon rescue. Total DNA was extracted from the WT strain PMB3(1) and the related Tn5 mutants using the protocol of Pospiech and Neumann (1995). The flanking Tn5-OT182 integration regions were identified using the rescue method as described previously (Deshazer et al. 1997). Briefly, 5 µg of DNA of each mutant was digested 4 h with *Eco*RI-HF in 50 µl. After heat inactivation, the digested DNA was ligated overnight in 25 µl. A volume of 10 µl was transformed into chemically competent *E. coli* DH5α and the transformants recovered on the appropriate selective medium. The resulting plasmids were extracted using the Miniprep kit from QIAGEN and sequenced with the primer pOT-RT at Eurofins MWG Operon (https://www.eurofinsgenomics.eu/). All enzymes for restriction digestion and ligation were purchased from New England Biolabs and were used according to the manufacturers' instructions. When required, PCR amplicons were purified using QIAquick PCR purification and gel extraction kits from QIAGEN. PCR was performed using Taq polymerase from 5PRIME.

Construction of pB2-*gdhC*, pB2-*resB* and pB2-*tatABC*. The ineffective MW phenotype of three Tn5-OT182 mutants of the strain PMB3(1) were complemented by expressing each

gene or region of interest (*gdhC*, *resB* and *tatABC*) in trans on plasmids pB2-*gdhC*, pB2-*resB* and pB2-*tatABC*. These genes/regions were amplified using specific primers (Table 1). The conditions for PCR involved a 5min denaturation step at 94°C, followed by 30 cycles of 94°C for 45s, melting temperature (Tm) for 45s, and 72°C for 2min30s. The Tm temperature was adapted according to the gene or region of interest. Each PCR product was purified and ligated into the pGEM-T Easy plasmid (Promega), and validated by Sanger sequencing (52). The gene *gdhC* was cloned as a *Kpn*I - *Spe*I fragment, the gene *resB* as a *Sac*I - *Spe*I fragment, and the *tatABC* genes as a *Sma*I - *Xba*I fragment into pBBR1MCS-2 (Kovach *et al*. 1995) to yield plasmids pB2-*gdhC*, pB2-*resB* and pB2-*tatABC* respectively. After verification by sequencing, the resulting constructs were transferred in chemically competent *E. coli* S17-1λpir and conjugated to the corresponding Tn5-OT182 mutant. The complemented mutants were selected on agar ABm medium supplemented with tetracycline and kanamycin. The presence of the intact gene in the complemented mutants was verified by a PCR using the appropriate primers (Table 1), the WT strain was the positive control and the mutant was the negative control. For each construction, a single transconjugant was conserved after validation and used in the different bioassays described below.

Analysis and quantification of organic acids. After a 4-day culture (25°C; 200 rpm) in liquid BHm amended with glucose (2 g/l) and devoid of iron, the supernatants of cultures of the WT and Tn5-OT182 mutants were recovered by centrifugation (10,000g during 15min). The supernatants were then filtered at 0.22 µm (GHP Acrodisc 25 mm syringe filter ; PALL) and stored at -20°C. Organic acid analyses were performed on an ion chromatography with conductivity detection (ICS 3000, Dionex Corp.) associated to an analytical column (IonPac® AS 11 HC, Dionex corp.) according to Balland *et al.* (2010). The supernatants were eluted with KOH solutions of varying concentrations (0.9-60 mM) over time (step gradient) with a

flow rate of 1.3 ml/min. Synthetic organic acids have used as references (sodium formate, D-gluconic acid, sodium butyrate, pyruvic acid sodium salt, sodium citrate tribasic, sodium oxalate, sodium propionate, sodium acetate, succinic acid disodium salt, DL-malic acid disodium salt, sodium-L-lactate and malonic acid disodium salt).

Analysis of the production of gluconate, 2KGA and 5KGA. Qualitative analysis was performed using thin layer chromatography (TLC) to identify which form of gluconic acid was produced by the WT strain PMB3(1). To do it, cultures were done in ABm medium supplemented with 10 g/l of glucose at 25°C and under shaking. After 4 days, the supernatant of culture was recovered and filtered at 0.22 µm (GHP Acrodisc 25 mm syringe filter; PALL). A volume of 4 µl for the standards and twice 4 µl for the culture supernatants were spotted on a Silica Gel 60 plate (Merck). After drying at room temperature, migration was performed in a solvent reagent containing ethyl acetate-acetic acid-methanol and deionized water (6:1.5:1.5:1). When the TLC plate was dried, spread with a freshly prepared revelation solution (diphenylamine (1 g) ; aniline (1 ml) ; acetone (50 ml) ; phosphoric acid (7.5 ml)). The treated TLC plate was then incubated at 120°C for 20 min to allow apparition of coloured spots. The results were analysed by measuring the retention factor (Rf) (corresponding to the distance moved by the sample divided to the solvent front) and the observation of the spot colour. The glucose, gluconate, 2KGA and 5KGA appeared as dark blue, pink, brown and dark purple spots, respectively. Solutions of glucose, gluconate, 2-keto gluconate and 5-keto gluconate adjusted at 100 mM were used as standard. In addition, gluconic acid was also quantified using an enzymatic bioassay (kit 10428191035 from r-biopharm/Roche), according to the manufacturer's instructions.

Screening of the Tn5-pOT182 mutant library. A first screening of the mutant library was done in microplates using liquid ABm medium supplemented with tetracycline. After 3-days culture, part of the cell suspension was spotted using a 96-well replicator on : i) solid TriCalcium Phosphate (TCP) to determine the MW ability of each Tn5-mutant and ii) modified liquid TCP medium (TCPm) to determine their acidification ability. These two bioassays are commonly used to determine the mineral weathering potential of bacterial strains (Calvaruso *et al.* 2007; Lepleux *et al.* 2013; Uroz *et al.* 2009b; Colin *et al.* 2017). In addition, the homogeneity of the $Ca_3(PO_4)_2$ in the TCP assays allow for a high throughput screening of mutant libraries. On the contrary, biotite is a heterogeneous material requiring important replication of the assay, making its use incompatible with a first screening of the mutant libraries. The solid TCP medium is composed per litter of : NH_4Cl 5 g ; NaCl 1 g ; $MgSO_4$ 1 g ; Glucose 10 g ; $Ca_3(PO_4)_2$ 4 g and 16 g of agar (pH 6.5). After incubation at 25°C for 7 days, the diameters of colonies and the diameter of discoloration zone (halo) were measured to determine the ability of each Tn5-mutant to solubilize inorganic phosphorous. The TCPm medium is modified version of the TCP devoid of $Ca_3(PO_4)_2$. The $Ca_3(PO_4)_2$ was removed from the medium to allow a better determination of the protons produced. The pH determination was performed after a 3-day incubation time. The supernatant was recovered by centrifugation (8,000 g for 15 min) and a volume of 180 µl was transferred to new microplates containing 20 µl of pH indicator (bromocresol green solution ; 1g/l), according to Uroz *et al*. (2007). The pH of the supernatant was determined at 595 nm using an automatic microplate reader (Bio-Rad, model iMark) and converted in pH values using a calibration curve (Uroz *et al.* 2007).

Functional assays done on Tn5-OT182 mutants impaired in their MW ability. After the first step of screening, all the Tn5-OT182 mutants presenting a significantly reduced halo of

solubilisation on solid TCP and/or a pH value significantly higher than the WT strain were tested in a calibrated way on different bioassays in order to generate quantitative and comparable data. The recovered Tn5-mutants were cultivated overnight in liquid LBm medium supplemented with tetracycline. The WT strain was used as a positive control. Ten milliliters of each culture was washed three times with sterile MQ-water to eliminate all medium traces. The absorbance at 595 nm of each resulting suspension was then adjusted at 0.95±0.03.

Phosphate solubilisation and solution acidification

Ten microliters of each calibrated suspension were then dropped in triplicates on the surface of the solid TriCalcium Phosphate (TCP) and in microplates containing the modified liquid TCP medium (TCPm). Measures of P solubilisation and of acidification were performed as described above (Colin *et al.* 2017).

Biotite dissolution

Five hundred microliters of the calibrated suspension of each strain was transferred into sterile glass tubes containing 4.5 ml of BHm medium (20 mg/l KCl; 150 mg/l $MgSO_4,7H_2O$; 80 mg/l $NaH_2PO_4,2H_2O$; 90 mg/l Na_2HPO_4, $2H_2O$; 65 mg/l $(NH_4)_2SO4$, 100 mg/l KNO_3; 20 mg/l $CaCl_2$) buffered at pH 6.5 and supplemented with glucose (2 g/l) and 100 mg of sterile biotite particles.

The biotite was obtained from Bancroft (Canada) and is a 2:1 phyllosilicate frequently found in acidic forest soils. This mineral holds K, Mg, and Fe nutrients. It is a pure homogeneous mineral, and its composition is as follows: 410.1 g/kg SiO_2, 109 g/kg Al_2O_3, 22.1 g/kg Fe_2O_3, 100.5 g/kg FeO, 2.7 g/kg MnO, 189 g/kg MgO, 4.1 g/kg Na_2O, 94.6 g/kg K_2O, 22.8 g/kg TiO_2, 44.2 g/kg F, and 0.8 g/kg Zn. Its structural formula is (Si_3Al_1) $(Fe^{3+}_{0.12}$

$Fe^{2+}_{0.61}$ $Mg_{2.06}$ $Mn_{0.02}$ $Ti_{0.13}$) and $K_{0.88}$ $Na_{0.06}$ O_{10} ($OH_{0.98}$ $F_{1.02}$). The particle size of biotite was calibrated from 200 to 500 µm.

Before use, all glass was rinsed with chloridric acid and deionised water to remove any chemical traces. The tubes containing the culture medium with biotite were then sterilised by autoclaving at 121°C. After seven days of incubation at 25°C (200 rpm), 1 ml of supernatant was sampled and centrifuged at 11,000g for 15 min and filtered at 0.22 µm. Quantification of the iron released from biotite and of the acidification of the medium were determined by adding 180 µl of supernatant of each culture in a new microplate containing 20 µl of ferrospectral or bromocresol green, respectively (Uroz *et a*l. 2007). The absorbance of these suspensions was measured at 595 nm and the data transformed in pH and iron concentrations using the colorimetric assays described above to determine the MW potential of each Tn5-pOT182 mutant.

In addition, model chelating (citric acid) or acidifying (hydrochloric acid) molecules were used as control in the same mineral weathering assay. Serial dilutions of citric acid (10^{-3} M; pH adjusted to 6 to 2) and hydrochloric acid (concentration adjusted to be at pH 6 to 2) were performed in BHm medium and incubated in the same condition than the bacterial strains tested as described in Uroz *et al.* 2007.

Cytochrome oxydase test

To test if mutants are affected in their cytochrome oxydase activity, 100 µl of the calibrated cell suspension were spotted on a filter paper and flooded in a 1% Tetramethyl-p-phenylenediamine (TMPD) solution during 10 min. After this incubation period, the filter paper was dried 30s and inspected. In the case of a positive reaction, the filter paper becomes purple, while in the case of a negative reaction it remains white (Kovacs, 1956).

290 *Glucose dehydrogenase (GDH) test*

291 To test if mutants were affected in their GDH activity, the test of Matsushita and Ameyama
292 (1982) was used on the calibrated cell suspension (CS) or on cell crude extract (CE). The cell
293 crude extract was obtained by ultra sonication treatment (Vibra-Cell; Sonics, Newtown USA)
294 of the CS, followed by a centrifugation at 7000 g (15 min) to remove intact cells and a
295 filtration at 0.22µm. A volume of 100µl of CS or CE was incubated with 100 µl of Tris-HCL
296 (50mM; pH:7.5), 10 µl of 2,6-dichlorophenolindophenol (DCIP; 6.7mM), 10 µl of phenazine
297 methosulfate (PMS; 20mM), 10 µl of (FAD; 600µM), 100µl of glucose (1M), and MQ water
298 in a final volume of 300 µL. The reaction is initiated by the addition of D-glucose. GDH
299 activity is measured at 600 nm in microplate reader (Tecan infinite M200 pro). Controls
300 without glucose and/or FAD were performed. In addition, a control without the CS or CE was
301 performed for each of the condition tested (+/- FAD; +/- Glucose).

302

303 *Growth assay and carbon substrate use*

304 To determine whether the mutants were impaired in their growth ability, tests were performed
305 under nutrient-rich and nutrient-poor conditions. For the nutrient-rich condition, 10 µl of each
306 calibrated suspension (WT and mutants) were added to 190 µl of liquid LB medium in a
307 microplate. The microplate was incubated at 25°C and orbital shaking during 4 days in a
308 microplate reader (Tecan infinite M200 pro). The absorbance was measured at 600 nm each 3
309 hour. For the nutrient-poor condition, 10 µl of each calibrated suspension was added to 190 µl
310 of liquid BHm medium amended with a source of carbon (2 g/l). The carbon sources used
311 were glucose, gluconic acid, 2-Keto-gluconate, 5-Keto-gluconate. After 5 days of incubation
312 at 25°C, the pH was measured with bromocresol green as described above and the growth was
313 measured at 595 nm.

314

315 **Bioinformatic analyses.** Genome analysis was performed using NCBI and MAGE (Vallen*et*
316 *et a*l. 2009). Homology search analysis and alignment were performed with BLAST (BlastN
317 and BlastP ; Altschul *et al.* 1997). Localization of the Tn5-OT182 insertion was done on
318 MAGE. A research of Twin Arginine Translocation (TAT) signal carrying proteins was done
319 using the predictor servers Tatfind (Dilk*s et al*. 2003) and TatP 1.0 (Bendtse*n et a*l. 2005).
320 The two proteins lists were assembled and analysed. Analyses of the pfam domains and of the
321 conservation of the GdhL subunit sequence were done using pfam (El-Gebal*i et al*. 2019) and
322 Seaview (version 4.5.4) (Gou*y et al*. 2010). To study the conservation of the GdhL sequence,
323 a set of 22 different genera or species related to *Collimonas* and available on international
324 databases were analysed among them, 11 were assigned to *Collimonas* genus (*Collimonas* sp.
325 PA-H2, OK242, OK307 and OK607, *C. fungivorans* Ter331 and Ter6*, C. arenae* Cal35,
326 Ter10 and Ter282*, C. pratensis* Ter91, Ter291). Other genera taxonomically close to
327 *Collimonas* were chosen : 2 belonging to the *Glaciimonas* genus (*Glaciimonas* sp. PCH181
328 and GS1), one to *Janthinobacterium,* 2 to *Herbaspirillum* (*H. rubrisubalbicans* and *H.*
329 *seropidecae*) and one to *Burkholderia cepacia*. In addition, we selected the sequences of the
330 large subunit of a set of GMC oxidoreductase which function was demonstrated: a gluconate
331 dehydrogenase (GADH ; BAH80545.1) and a sorbitol dehydrogenase (BAD60913.1) from
332 *Gluconobacter frateurii* (Toyam*a et al*. 2005; Saichan*a et al*. 2009), a fructose dehydrogenase
333 large subunit of *Gluconobacter japonicas* (BAM93252.1) (Kawa*i et a*l. 2013). We also
334 considered the sequences of the large subunit of a putative sorbitol dehydrogenase from
335 *Gluconobacter oxydans* H24 (AFW02570.1) and a dehydrogenase subunit from *Pantoea*
336 *agglomerans* (AAF21261.1). The same genome resources were also used to recover the pqq-
337 genes as well as the pqq-dependent enzymes.
338

Statistical analysis. Statistical analyses were performed in R software. Data shown were means of, at least, triplicates. Differences between sample's means were analysed by ANOVA and Tukey HSD tests.

Nucleotide sequence accession number. The nucleotide sequence reported in this paper are related to the genome sequence of the strain PMB3(1), which has been deposited in the GenBank database under accession no. WXXL00000000.

RESULTS

1) Genomic and physiological characterization

At the genomic level, the detailed analysis of the genome of strain PMB3(1) did not permit to evidence any PQQ-dependent GDH nor the presence of the PQQ cofactor encoding genes. Similarly, none of the *Collimonas* genome available in the international databases (*i.e.*, *Collimonas* sp. PA-H2, *C. fungivorans* Ter331 and Ter6*, C. arenae* Cal35, Ter10 and Ter282*, C. pratensis* Ter91, Ter291) possess PQQ encoding genes and/or PQQ-dependent enzymes, suggesting that alternative MW pathways exist in collimonads.

At the chemical level, high concentrations of gluconic acid were detected in the supernatant of cultures of strain PMB3(1) done with glucose (Table 2), evidencing that this strain was capable of converting glucose to gluconic acid (GA) through an alternative, PQQ-independent pathway. Noticeably, the thin layer chromatography analyses confirmed the large production of gluconic acid, but also a weak production of 2 keto-gluconic acid (2KGA) by strain PMB3(1) as evidenced by the comparison with the migration retention factor (Rf) and the colour of the synthetic GA and 2KGA controls used (Fig. 1; Table 2). A kinetic analysis confirmed the continuous accumulation of GA, while 2KGA was hardly detectable. Interestingly, the growth assays done in minimal medium supplemented with a single source

of carbon (*i.e*., glucose, GA, 2KGA or 5KGA) confirmed that glucose, GA and 2KGA were used as carbon source by strain PMB3(1), but not 5KGA. Among them, glucose was the sole carbon which metabolism allowed an acidification of the culture supernatant (pH=3.5), while the pH did not change in presence of GA and 2KGA (*i.e.,* pH=6.2).

2) Isolation of mutants affected in the ability to solubilize inorganic phosphorous

The first high throughput screening of the mutant library allowed us to recover a total of 4 mutants (*i.e*., 25(10F), 31(11B), 34(11H), 59(7B)) impaired in their ability to solubilize inorganic phosphorous (Pi).

The use of the calibrated procedure (see materials and methods) confirmed that these 4 mutants were significantly altered in their ability to solubilize Pi ($P<0.05$). Based on this second screening, three of these mutants, 25(10F), 31(11B), 34(11H), did not present a solubilisation halo (Table 2). For the mutant 59(7B), a reduction of 34% of the halo diameter was observed compared to the WT strain (halo_WT: 0.79 cm ± 0.04 vs halo_59(7B): 0.52 cm ± 0.1). All these mutants and WT presented similar colony diameters. The acidification assay revealed that the ability of mutants 25(10F), 31(11B) and 34(11H) to acidify was significantly reduced ($P<0.05$). Indeed, while the WT strain and mutant 59(7B) acidified the medium from the initial pH 6.5 to pH 3.7 in three days, mutants 25(10F), 31(11B), 34(11H) acidified the medium only to *c.a*. pH 4.7 (average value).

3) Ability to weather biotite

The ability to weather a complex mineral was tested only for the three mutants totally impaired in their ability to solubilize Pi (*i.e.*, 25(10F), 31(11B), 34(11H)) as well as for the WT strain (Fig. 2). After a 7-day incubation in presence of glucose as carbon source, the WT strain was able to release 1.29 ± 0.13 mg/l of iron in the solution. In comparison, the three

mutants 25(10F), 31(11B) and 34(11H) released significantly less iron (0.32 ± 0.08, 0.54 ± 0.04 and 0.39 ± 0.02 mg/l, respectively) ($P<0.05$) (Fig. 2A). Those values corresponded to a maximal reduction of 75% for mutant 25(10F) and a minimal reduction of 58% for mutant 31(11B) compared to the WT strain. After the 7-day incubation, the WT strain decreased the pH of the culture supernatant to pH=3.3 ± 0.1, while the mutants reached significantly higher value (4.3 to 4.5; $P<0.05$) (Fig. 2B). The co-visualization of the quantity of iron released from biotite and of the pH of the supernatant confirmed the strong perturbation of the mineral weathering ability of the mutants compared to the WT strain (Fig. 2C).

4) Sequence analyses of the genomic region for the different mutants

The genomic region flanking the plasposon insertion of each mutant was isolated by self-cloning using the plasposon rescue method. For each mutant, 3 independent clones were recovered, sequenced and blasted against the genome sequence of strain PMB3(1). This revealed a single genomic region per mutant, demonstrating a unique plasposon insertion event in each of the mutants considered [25(10F), 31(11B), 34(11H), 59(7B)]. The sequences were also blasted against nucleic acid and protein databases of the NCBI for homologous sequences.

In mutant 25(10F), the plasposon is inserted in a gene we named *gdhC* (NKI70796.1). This gene presented high homology with a cytochrome c subunit of a Glucose/Gluconate/Sorbitol 2-dehydrogenase (Fig. 3, Table 3). Pfam analysis highlighted two conserved domains (cytochrome c from 36 to 137 aa/ cytochrome CBB3 from 322 to 406 aa ; e-value = 6.6e-07 /5.4e-10, respectively) corresponding to a cytochrome c oxidase protein. This gene is preceded by two genes presenting sequence homology with subunits of a Glucose/Methanol/Choline (GMC) oxidoreductase. The first one presented high sequence homology (98 %) with the large subunit (NKI70795.1; *gdhL*) belonging to the FAD

flavoprotein oxidoreductases, while the next gene presented high homology (80 %) with the gamma subunit (NKI70794.1; *gdhS*) of a Sorbitol/Glucose/2-Keto-D-Gluconate dehydrogenase. Pfam analysis revealed that this gamma subunit presented high sequence similarities with the FAD-Sorbitol dehydrogenase family protein (e-value = $2.5.10^{-48}$) and carried a potential TAT-signal.

In mutant 31(11B), the plasposon is inserted in a genomic region presenting high sequence homology with a *resB* homologous gene (NKI71673.1 ; 94% identity with cytochrome c biogenesis protein ResB in *Collimonas sp.* PA-H2) (Fig. 3, Table S1). This gene belongs to a genetic structure composed of 3 genes (NKI71672.1; NKI71673.1 ; NKI71674.1) involved in cytochrome c biogenesis /maturation. Among them, gene NKI71672.1 codes for a cytochrome c4 immature protein and gene NKI71673.1 is gene *resC* coding for a cytochrome c biogenesis protein. In the vicinity of the *resB* gene, two other genes, *yedY* and *yedZ* (NKI71676.1, NKI71677.1), presenting high sequence homology with a sulfite oxidase were detected.

In mutant 34(11H), the plasposon is inserted in a genomic region presenting high sequence homology with the Twin Arginine Translocation pathway (TAT) operon (*tatABC*). The insertion was localized between the gene *tatB* (NKI71758.1; 93% identity with Sec-independent protein translocase subunit TatB in *Collimonas sp.* PA-H2) and *tatC* (NKI71759.1; 95% of identity with the twin-arginine translocase subunit TatC in *Collimonas sp*. PA-H2) (Fig. 3, Table S2).

In mutant 59(7B), the plasposon is inserted in the gene *int* (NKI72639.1) presenting high sequence homology with an apolipoprotein N-acyltransferase (92% of identity with the apolipoprotein N-acyltransferase of *Collimonas sp.* PA-H2) (Fig. 3, Table S3). This enzyme is responsible for the last step of lipoprotein maturation. In the vicinity of this gene, 5 genes involved in metabolism and two genes involved in information storage and processing were identified according to their COG class.

5) Identification of TAT-dependent proteins

Due to the localization of the plasposon insertion of mutant 34(11H) in the TAT system region, a bioinformatic analysis was done to identify all proteins presenting a putative TAT signal in the genome of strain PMB3(1). Indeed, the perturbation of the MW ability may be related to a protein carried by the TAT system. This screening allowed the identification of 74 TAT-proteins related to different Clusters of Orthologous Groups (COG) (metabolism, cellular processes and signalling, information storage and processing, or poorly characterized (Table S4; Fig. S1). Among them, we noticeably identified the protein *gdhS* that corresponds to the gamma subunit of the Sorbitol/Glucose/2-Keto-D-Gluconate dehydrogenase gene (NKI70794.1). This gene is in an operon along with gene *gdhC* (*i.e.*, cytochrome subunit of the Sorbitol/Glucose/2-Keto-D-Gluconate dehydrogenase) interrupted in mutant 25(10F) (see fig. 3) Other enzymes related to putative alkaline phosphatases (*i.e.*, PhoD like, NKI71510.1 and NKI72605.1), involved in cytochrome c biogenesis (NKI72023.1) or presenting an oxidoreductase activity (NKI71676.1) were also identified in the list of TAT-proteins.

6) Functional and physiological characterization of mutants 25(10F), 31(11B) and 34(11H)

Cytochrome activity

As mutants 25(10F) and 31(11B) were affected on genes encoding a cytochrome subunit or involved in the biogenesis of cytochrome c, a cytochrome oxidase test was performed on all mutants. This qualitative test based on the oxidation of Tetramethyl-p-phenylene diamine (TMPD) revealed that the three mutants formed a purple pigment as the WT strain (Table 2), revealing that the cytochrome c oxidase of the strain PMB3(1) was still functional in all the mutants. This result highlights that strain PMB3(1) possesses several cytochrome c biogenesis

463 systems independent on the resB/resC system interrupted in mutant 31(11B). Indeed, a
464 genome analysis revealed that the strain PMB3(1) possesses two cytochrome biogenesis loci.
465
466 *Detection and quantification of organic acids*
467 Ionic chromatography analyses permitted to identify the main acids produced (i.e., Gluconate,
468 oxalate, pyruvate, formate, and succinate) by the WT strain and mutants in presence of
469 glucose (Table 2). Gluconate was the major organic acid detected in the WT culture
470 supernatant, reaching a concentration of 878.7±3.3 mg/l, while all other organic acids are
471 present at very low concentrations (pyruvate: 2.87 mg/l; succinate: 0.07 mg/l). Noticeably,
472 gluconate was not detected in any of the supernatants from the 3 mutants (*i.e.*, mutants
473 25(10F), 31(11B) and 34(11H); Table 2). Amongst other organics, only pyruvate presented
474 significant differences between the WT strain and mutants, but with very low concentrations
475 (WT: 2.87±0.63 mg/l; 25(10F): 1.08± 0.03 mg/l; 31(11B): 1.55±0.23 mg/l and 34(11H):
476 0.11±0.06 mg/l) ($P<0.05$).
477
478 *Growth in rich (LB) medium*
479 To get a better understanding of the importance of the gene(s) interrupted in the different
480 mutants, their growth was monitored for 120 hours in LB medium (Fig. 4; Table 2). No
481 difference between the WT and the 25(10F) mutant was observed. Indeed, the growth rate
482 (0.09 ± 0.02 h^{-1}; $P<0.01$), the lag time (ca. 10 h), the maximal growth yield (OD_{595nm} of $1.20 \pm$
483 0.05) as well as the time necessary to reach the stationary phase for the WT and mutant
484 25(10F) (*i.e.*, 40 h) were similar. In contrast, mutants 31(11B) and 34(11H) differed
485 significantly from the WT strain. Mutant 31(11B) presented a growth rate of 0.06 ± 0.01 h^{-1}, a
486 lag phase of 25 h, a maximal growth yield (OD_{595nm}) of 0.95 ± 0.08 and it required 50 h to
487 reach the stationary phase. Mutant 34(11H) presented the lowest growth rate of 0.02 ± 0.01 h^{-}

488 [1], a maximal growth yield (OD_{595nm}) of 1.08 ± 0.08 and it required 120 h to reach this
489 maximum.
490
491 *Impact of the carbon source on the acidification process*
492 As acidification plays an important role in the mineral weathering process by strain
493 PMB3(1), several carbon sources coming from the metabolism of glucose (*i.e.*, gluconate,
494 2KGA, 5KGA) were tested in minimal medium (BHm) (Fig. 5). Contrary to the strong
495 acidification observed with glucose, these growth assays revealed no difference of pH
496 between the WT and mutant strains when they were cultivated in minimal medium amended
497 with glucose derivatives such as GA or 2KGA (pH_{WT} = pHmutant = 6.2). No growth was
498 observed with 5KGA.
499
500 ***7) Complementation analysis of the mutants***
501 To confirm the involvement of the interrupted genes identified in the different mutants (*i.e.*,
502 25(10F), 31(11B) and 34(11H)) in the MW ability of strain PMB3(1), a functional
503 complementation was performed. For each mutant, the native gene(s) under a constitutive
504 promoter was cloned in the pBBR1MCS-2 vector. These constructions were then transformed
505 in the corresponding mutant and tested with the same set of functional assays as described
506 above. Noticeably, the quantitative assays performed on solid TCP medium revealed that the
507 complemented mutants 25(10F)(pB2-*gdhC*) and 34(11H)(pB2-*tatABC*) recovered fully their
508 mineral weathering ability to WT effectiveness (Table 2). The mutant 31(11B)(pB2-*resB*) was
509 restored in its ability to weather mineral, but presented a slightly lower efficiency than the
510 WT strain, when harbouring gene *resB* on the pBBR1MCS-2 plasmid. Regarding
511 acidification, upon complementation pH was further reduced from pH 5.1 ± 0.1 observed in
512 the mutants to 4.4 ± 0.1 in the complemented mutants after 3 days, which was not

513 significantly different from that observed with the WT strain harbouring the empty vector
514 pBBR1MCS2 (4.3 ± 0.1). In addition, the restoration of the glucose dehydrogenase activity
515 was observed in the complemented mutants. Last, complementation restored growth of all
516 mutants (Fig. 4).
517
518 ***8) Bioinformatic properties and conservation of GMC oxidoreductases in the collimonads***
519 ***and related genera***
520 For bacteria carrying a glucose dehydrogenase enzyme of the GMC oxidoreductase family,
521 the conversion of glucose to gluconic acid is mainly performed by the large subunit (*i.e.*,
522 *gdhL*) of the enzyme (Yamaoka *et al.* 2008). In this context, bioinformatic analyses were
523 performed on this subunit to analyse its properties and its conservation among collimonads
524 and related taxa.
525 In strain PMB3(1), this approach allowed to identify a single GMC oxidoreductase
526 organized in three subunits and corresponding to the genomic region described above for
527 mutant 25(10F). A second homologous of the large subunit (GdhL) was also identified in
528 strain PMB3(1), but with a low identity (20%). Contrary to the GMC oxidoreductase, this
529 homologue is organized as a single unit (*i.e.*, one gene) and encodes a putative choline
530 dehydrogenase. The pfam analysis done on the sequence of the large subunit of the strain
531 PMB3(1) evidenced the presence of a Rossmann-like domain (amino acid 11 to 41; e-value =
532 2.0e-5) and two GMC oxidoreductase domains (domain C: 405 to 525, e-value 1.5e-18;
533 domain N: 176 to 318, 1.5e-5), supporting by this way the function attributed to the gene
534 identified in our study (*i.e.*, a Glucose dehydrogenase from the GMC oxidoreductase family)
535 (Fig. S2). Notably, all the GMC oxidoreductases described in the literature present the 3
536 domains detected (Rossmann, GMC_N, GMC_C) and all are specifically associated to
537 enzymes binding FAD as cofactor (*i.e.*, gluconate dehydrogenase, GADH; glucose

dehydrogenase, GDH; fructose dehydrogenase, FDH; sorbitol dehydrogenase, SDH) (Kataoka *et al.* 2015; Toyama *et al.* 2005).

The comparison of homologous sequences from the available *Collimonas* genome sequences revealed a very good conservation of the different domains (Fig. S3). In the putative FAD domain, only two positions on a total of 31 varied among the collimonads (Fig. S2). In the GMC_C domain, 10 positions on a total of 86 varied, while 16 positions on a total of 121 varied in the GMC_N domain (Fig. S2). Beside these pfam domains, we also detected in the large subunit sequence of strain PMB3(1), the cysteine-rich region (cys208, cyst214, cys218 in our alignment; Fig. S2) identified by Shiota *et al.* (2016) as specific of the FAD-dependent dehydrogenases. This region is constituted by three conserved cysteine (Cys) residues (**C**CGNNN**C**MPI**C**P), all conserved in the *Collimonas* genomes considered. This particular site constitutes an iron-sulfur cluster essential for electron transfer from FAD to the cytochrome c subunit (Shiot*a et a*l. 2016).

When the sequence comparison integrated neighbouring genera, it revealed a good conservation of the large subunit sequence among the taxa tested and a stronger relatedness of *Janthinobacterium* and *Glaciimonas* with *Collimonas*. In contrast, *Herbaspirillum* presented important variations (Fig. S3). The sequence of the GdhL protein of strain PMB3(1) presented ca. 90 % of identity with that of strains PCH181 and GS1 of *Glaciimonas* sp., 80 % with that of *Janthinobacterium* and only 50 % with that of *Herbaspirillum seropedicae* and *H. rubrisubalbicans*. The low relatedness of the GdhL of *Herbaspirillum* was also visible in the sequence alignment, especially in the domain GMC_C.

Last, a sequence comparison between the large subunit of strain PMB3(1) and the large subunit of FAD-dependent dehydrogenases for which the function and/or the FAD-dependence were experimentally demonstrated (*i.e.*, a GADH from *Gluconobacter frateurii*, two SDHs from *Gluconobacter oxydans* and *G. frateurii,* a FDH from *Gluconobacter*

japonicas and a GDH from *Burkholderia cepacia*) or suspected (choline dehydrogenase (CDH) from *Pantoea agglomerans*) was performed (Fig. S3). This analysis revealed that the most distantly related sequence was the GADH. The positions on the phylogenetic tree are supported by the strong sequence variations observed in the sequence alignment. The large subunit sequence of strain PMB3(1) appeared also poorly related to the FDH and SDH. The stronger relationship was observed with the glucose dehydrogenase (GDH) from *Burkholderia cepacia* (Tsuya *et al.* 2006).

DISCUSSION

The ability to weather minerals was evidenced for a broad range of bacterial genera, but the genes involved have been poorly investigated and characterized. To date, the main system described is related to the PQQ-dependent glucose dehydrogenases (PQQ-GDH), which allows the production of protons and gluconic acid. The role of such enzymes and the related *pqq* genes (*i.e.*, *pqqABCDEF*) in the solubilisation of highly weatherable minerals (*i.e.*, Pi) was reported in several studies (Goldstein, 1995; Goldstei*n et a*l. 2003; Babu-Kha*n et* al. 1995), but only recently for a complex mineral (*i.e.*, biotite; Wang *et al.* 2020). In this study, we investigated the molecular mechanisms and the genes explaining the high MW effectiveness of strain PMB3(1) of *Collimonas* as well as their relative conservation among collimonads.

Collimonads have been isolated from various nutrient-poor environments (*i.e.*, sand dune, forests soil) and in fungal rich habitats (*i.e.*, mycorrhizosphere) (Colin *et al.* 2017; Uroz *et al.* 2007; Lepleux *et al.* 2012). They are recognized as particularly effective at mobilizing nutrients using fungal derived metabolites such as glucose, trehalose, mannitol (Uroz *et al*. 2009b). The genome analysis performed in this study reveals that none of the sequenced *Collimonas* to date possess the canonical *pqq* biosynthesis genes nor PQQ-dependent

588 enzymes, meaning that alternative mechanisms to the PQQ-dependent pathway are involved
589 in their MW ability. Those results confirmed the observations made on the Ter *Collimonas*
590 strains (Ter331, Ter14, Ter6, Ter91 or Ter10; Mela *et al.* 2012) or on strain PMB3(1) (Picard
591 *et al.* 2020). In this study, we confirmed that strain PMB3(1) is very effective at weathering
592 and at producing gluconic acid, and we showed for the first time that at least a part of this
593 gluconic acid is converted to 2-keto-gluconic acid (2KGA), evidencing the presence of a
594 glucose dehydrogenase (GDH) activity and of a gluconate dehydrogenase (GADH) activity.
595 Such conversion of glucose to gluconic acid and then to 2KGA corresponds to the direct
596 oxidative pathway described by Eber*t et a*l. (2011). The 2KGA is then converted into 6-P-
597 gluconate by a 2-keto gluconate kinase and a 2-keto gluconate 6-phosphate reductase prior to
598 entering the Pentose pathway or the Entner-Doudoroff pathway (Eber*t et a*l. 2011). Beside its
599 capability to produce gluconic and 2-keto-gluconic acids, we demonstrated that strain
600 PMB3(1) is capable of metabolizing these two acids, without acidification of the solution. No
601 growth was observed with the 5-keto-gluconic acid. The ability to produce GA and 2KGA is
602 well conserved among Gram-negative bacteria, but the production of 5KGA or 2,5KGA is
603 more specific to acetic bacteria such as *Acetobacter* or *Gluconobacter* (Sützl *et al.* 2019).
604 Bacteria producing GA and 2KGA have been described as being more effective at
605 solubilizing calcium phosphate than other bacteria (Babu-Khan *et al.* 1995).

606 A focus on the genomic region flanking the plasposon insertion in mutant 25(10F) allowed
607 a better understanding of the link between the 3 weathering null mutants, though they were
608 geographically distant and apparently unrelated. We identified a PQQ-independent enzyme
609 presenting high homology with Glucose/Methanol/Choline (GMC) oxidoreductases (Sützl *et*
610 *al.* 2019; Cavener, 1992). The GMC superfamily encompasses a wide variety of FAD-
611 dependent oxidoreductases (*e.g.*, glucose oxidase (GO), glucose dehydrogenase (GDH),
612 alcohol oxidase (AO), cellobiose dehydrogenase (CDH)) that are present in both prokaryotic

and eukaryotic domains (Sützl *et al.* 2019; Zamocký *et al.* 2004). They are composed of three subunits encoding a small subunit, a large subunit, and a cytochrome c subunit (Sützl *et al.* 2019; Cavener, 1992), corresponding exactly in term of organization (small subunit: *gdhS*; large subunit: *gdhL* and cytochrome subunit: *gdhC*) and sequence homology to the genomic region impacted in mutant 25(10F). The large subunit of strain PMB3(1) is characterized by several domains according to pfam analysis (a FAD domain and two GMC oxidoreductase domains (N and C)) and the presence of a cysteine rich region. This cysteine rich region was shown to be conserved in the catalytic large subunit of FAD-dependent dehydrogenases (Shiota *et al.* 2016). While we were able to demonstrate the GDH activity and the production of gluconic acid by strain PMB3(1), testing experimentally the FAD dependence of the GDH activity would require the purification of the three subunits in a functional form, which was not possible in our labs. A FAD dependence test performed on lyzed cells was inconclusive. The known FAD-dependent GDHs are involved in the oxidation of different substrates including sugars, alcohols, cholesterol and choline and their conversion to the corresponding lactone. In presence of glucose, these enzymes allow the production of D-glucono-1,5-lactone, which is then converted to gluconic acid through the action of a gluconolactonase or spontaneous hydrolysis (Ferr*i et a*l. 2011; Zamocký *et al*. 2004). Strain PMB3(1) possesses several putative gluconolactonases (NKI70323.1, NKI67822.1, NKI72143.1) in its genome. Although additional experiments are required to support the different steps, we proposed here a hypothetical functional model of the main mechanisms used by strain PMB3(1) to weather minerals and linking the different mutants obtained in this study (Fig. 6).

To be functional GMC oxidoreductases also require a mature cytochrome c subunit and a small subunit. The maturation of the cytochrome c subunit is performed through the ResB and ResC system (Crow *et al.* 2005), which allows the translocation of the heme during cytochrome maturation (Kranz *et al.* 2009). Without the heme, the cytochrome c subunit is

not functional and does not permit electron transfer. Strain PMB3(1) possesses both ResB and ResC system and very interestingly the *resB* gene is interrupted in our mutant 31(11B), likely interrupting the maturation of the cytochrome c subunit of the GDH identified. Notably, its activity was restored when a complementation in *trans* was done with the gene *resB*. The last small subunit of the GMC oxidoreductases is a protein required for the proper folding and secretion of the large subunit (Shiota *et al.* 2016; Yamaoka *et al.* 2008). Indeed, without a functional small subunit, the GDH of *Burkholderia cepacia* strain SM4 failed to perform the oxidation of its substrate (Yamaoka *et al.* 2008). The small subunit of strain PMB3(1) is also characterized by a TAT-signal. This particularity was also observed in various dehydrogenases organised in three subunits. This strongly suggests that in absence of translocation of the small subunit, the related FAD-dependent enzyme is not functional. Congruent with this hypothesis, Toyama *et al*. (2007) showed that the assembly of the different subunits of the FAD-GADH of *Gluconobacter dioxyacetonicus* was performed in the cytoplasm before the translocation through the TAT system and using the TAT signal of the small subunit. In addition, experimentations showed that TAT system allowed the translocation of folded proteins associated with their co-factor (Allen *et al.* 2002; Palmer and Berks, 2012). In this context, the TAT-signature of the PMB3(1) GdhS (*i.e*., the small subunit of the GDH) represents the link between the mutant 34(11H) and the MW null phenotype. Besides the small subunit of the Glucose dehydrogenase (GdhS) of strain PMB3(1), several other TAT-exported proteins could also play a role in MW, such as those involved in cytochrome biogenesis, oxidoreduction or more especially in the hydrolysis of organic phosphate (Table S4) (Chhabra *et al.* 2013 ; Lidbury *et al.* 2016). However, the complete loss of MW activity in the other two mutants (*i.e.,* 25(10F), 31(11B)) would not support this hypothesis.

662 The conservation of the MW ability among collimonads prompted us to determine the
663 phylogenetic distribution of the GDH type identified in strain PMB3(1) in collimonads and
664 closely related genera. The comparison done on the sequenced genomes of *Collimonas* (*C.*
665 *pratensis* , *C. arenae*, *C. fungivorans*, *C.* sp.) revealed a good conservation of this GDH type
666 as well as of the TAT system, and the absence of PQQ-dependent GDHs or the related *pqq*
667 biogenesis genes in collimonads. Such conservation of the PQQ-independent GDH identified
668 from strain PMB3(1) was expected, as *Collimonas* are known to harbour important gene
669 conservation among the different species described (Mela *et al.* 2012). The comparison done
670 between the large subunit of the GDH of strain PMB3(1) and other dehydrogenases FAD-
671 dependent in other taxa revealed that it was more strongly related to *Glaciimonas*,
672 *Janthinobacterium* and *Burkholderia* than *Herbaspirillum* or *Gluconobacter*. The GDH of
673 PMB3(1) presented higher homology with other alcohol dehydrogenases experimentally
674 identified as sorbitol (FW02570.1), glucose (AAN39686.1) or fructose (BAM93252.1)
675 dehydrogenases, all FAD-dependent. This relative proximity between different type of FAD-
676 dependent dehydrogenases may be due to the low substrate specificity of some of these
677 enzymes, which are capable of oxidizing different substrates, including glucose (Yamaoka *et*
678 *al.* 2008). In contrast, the most distantly related FAD-dependent dehydrogenase of our
679 analysis was the GADH (*i.e.*, Gluconate DH; BAH80545.1) of *Gluconobacter frateurii* that
680 converts gluconate to 2 ketogluconate. Beside the large subunit, the small and cytochrome
681 subunits were also well conserved between collimonads and related taxa. The conservation of
682 an homologous of the GDH of strain PMB3(1) in *Glaciimonas* and the presence of this taxa in
683 nutrient-poor and rocky environments (*i.e*. the forest soil, alpine glaciers) (Udovičić *et al.*
684 2015) suggest that members of this genus are well adapted to oligotrophic conditions and
685 capable of weathering minerals as are collimonads. Their MW ability remains to be tested. In
686 contrast, important differences were found in the sequence of the GMC_C domain and the

Cys-rich region of the large subunit of *Herbaspirillum*, a genus reported as non- or poorly-effective at weathering minerals (Uroz *et al.* 2009b). Beside the presence of a GMC oxidoreductase homologue, our genomic analyses revealed that some representative strains of the genus *Burkholderia*, *Glaciimonas*, *Gluconobacter* or *Pantoea* were also characterized by the presence of *pqq*-encoding genes as well as PQQ-dependent enzymes in their genome, but their ability to solubilize minerals is unknown. Such results reveal that bacteria can possess both PQQ-dependent and -independent GDH. Interestingly, a dual transcriptomic and proteomic approach done on another effective MW bacterial strain (i.e. strain PML1(12) of *Caballeronia mineralivorans*) harbouring both systems highlighted that a homologous GMC oxidoreductase was up-regulated in presence of biotite, while the *pqq*-related genes appeared poorly expressed and not regulated (Uroz *et al*. 2020). This GMC oxidoreductase presented high sequence homology with the FAD-dependent GDH of *Burkholderia cepacia* strain SM4 and with the GDH identified in strain PMB3(1) in our study, suggesting that such enzyme may be broadly conserved in Burkholderiales.

CONCLUSION

This study elucidated the main molecular mechanism used by collimonads to weather mineral. Our results show that their effective MW ability is likely due to an enzymatic activity based on a PQQ-independent GMC-DH capable of oxidizing glucose to gluconic acid (*i.e.*, a PQQ-independent glucose dehydrogenase). This crucial step of the direct oxidative pathway leads to a high production of protons jointly with the oxidation of glucose and an important acidification of the nearby environment and consequently the dissolution of the minerals. This enzyme appears conserved among collimonads explaining their conserved effectiveness. The variations of sequence observed in the GMC_C domain of the large subunit of this enzyme may explain why some of the related taxa (*i.e*., *Herbaspirillum*, *Janthinobacterium*) harbour a

lower effectiveness at weathering minerals than collimonads. Our results represent the first demonstration that MW in bacteria is not exclusively explained by the PQQ-dependent GDH production of gluconate and that an alternative pathway based on a PQQ-independent GDH also exists in MW bacteria lacking the PQQ system. As such enzyme is largely distributed in Bacteria, Archaea and in some Eukaryotes (Sützl *et al.* 2019), it may open new perspectives in the understanding of the MW process by microorganisms and plants. Noticeably, our genomic analyses revealed that some bacteria harbour both the PQQ-dependent and PQQ-independent GDH in their genome as stated in some representative strains of the genus *Burkholderia*, *Glaciimonas*, *Gluconobacter* or *Pantoea* (this study; Uroz *et al.* in press). The next step for future researches will be to determine whether i) the GDH activity is regulated by the availability of inorganic nutrients (P, K, Mg…) as is the case for the PQQ-dependent GDH (Sasnow *et al.* 2016) or the presence/absence of a mineral (Uroz *et al.* 2020) and ii) the GDH genes can be used as biomarkers of the presence of the mineral weathering function into the soil.

ACKNOWLEDGMENTS

This work was supported by grants from the EC2CO program and the Labex ARBRE to S.U. L.P. was also supported by a fellowship from the French Ministère de l'Enseignement Supérieur, de la Recherche et de l'Innovation. The UMR1136 and UR1138 are supported by the ANR through the Laboratory of Excellence Arbre (ANR-11-LABX-0002-01). The authors thank Dr. P. Frey-Klett for helpful discussions, E. Morin for bioinformatics support and the MICROSCOPE team (Genoscope) for the support provided on the genome of strain PMB31.

REFERENCES

737 Alder NN, Theg SM. Energetics of protein transport across biological membranes: A study of
738 the thylakoid delta pH-dependent/cpTat pathway. *Cell Press*. 2003;112:231–242.
739 Allen SCH, Barrett CML, Ray N, Robinson C. Essential cytoplasmic domains in the
740 *Escherichia coli* TatC protein. *J Biol Chem.* 2002;277:10362–10366.
741 Altschul SF, Madden TL, Schaffer AA, Zhang J, Zhang Z, Miller W and Lipman, DJ. Gapped
742 BLAST and PSI-BLAST: a new generation of protein database search programs. *Nucleic*
743 *Acids Res.* 1997; 25:3389–3402.
744 Babu-Khan S, Yeo TC, Martin WL, et al. Cloning of a mineral phosphate-solubilizing gene
745 from *Pseudomonas cepacia*. *Appl Environ Microbiol* 1995;61:972–978.
746 Balland C, Poszwa A, Leyval C, Mustin C. Dissolution rates of phyllosilicates as a function
747 of bacterial metabolic diversity. *Geochim Cosmochim Acta* 2010; 74:5478–5493.
748 Bendtsen J, Nielsen H, Widdick D, Palmer T, Brunak S. Prediction of twin-arginine signal
749 peptides. *BMC Bioinformatics* 2005; 6:167.
750 Bonneville S, Smits MM, Brown A, *et al.* Plant-driven fungal weathering: Early stages of
751 mineral alteration at the nanometer scale. *Geology*. 2009; 37:615-618.
752 Brantley SL. Kinetics of Mineral Dissolution, p. 151–210. In Brantley, SL, Kubicki, JD,
753 White, AF (eds.), Kinetics of Water-Rock Interaction. 2008; Springer New York, New York,
754 NY.
755 Calvaruso C, Mareschal L, Turpault M-P, Leclerc E. Rapid clay weathering in the rhizosphere
756 of norway spruce and oak in an acid forest ecosystem. *Soil Sci Soc Am J.* 2009; 73:331–338.
757 Calvaruso C, Turpault M-P, Frey-Klett P. Root-associated bacteria contribute to mineral
758 weathering and to mineral nutrition in trees: a budgeting analysis. *Appl Environ Microbiol*.
759 2006; 72:1258–1266.
760 Calvaruso, C., Turpault, M. P., Leclerc, E., Ranger, J., Garbaye, J., Uroz, S., & Frey-Klett, P.
761 Influence of forest trees on the distribution of mineral weathering-associated bacterial

762 communities of the *Scleroderma citrinum* mycorrhizosphere. *Appl Environ Microbiol.*
763 2010;76:4780-4787.
764 Cavener DR. GMC oxidoreductases: A newly defined family of homologous proteins with
765 diverse catalytic activities. *J Mol Biol.* 1992; 223:811-814.
766 Chhabra S, Brazil D, Morrissey J, Burke JI, *et al.* Characterization of mineral phosphate
767 solubilization traits from a barley rhizosphere soil functional metagenome. *Microbiol Open*
768 2013; 2:717–724.
769 Chilton M-D, Currier TC, Farrand SK, Bendich AJ, *et al. Agrobacterium tumefaciens* DNA
770 and PS8 bacteriophage DNA not detected in crown gall tumors. *Proc Natl Acad Sci*
771 1974;71:3672–3676.
772 Colin Y, Nicolitch O, Turpault M-P, Uroz S. Mineral types and tree species determine the
773 functional and taxonomic structures of forest soil bacterial communities. *Appl Environ*
774 *Microbiol*. 2017; 83:e02684-16.
775 Collignon, C., Uroz, S., Turpault, M. P., & Frey-Klett, P. (2011). Seasons differently impact
776 the structure of mineral weathering bacterial communities in beech and spruce stands. *Soil*
777 *Biol and Biochem.* 2011;43:2012-2022.
778 Crow A, Le Brun NE, Oubrie A. The role of ResA in type II cytochrome c maturation.
779 *Biochem Soc Trans.* 2005; 33:149–151.
780 Dennis JJ, Zylstra GJ. Plasposons: modular self-cloning minitransposon derivatives for rapid
781 genetic analysis of Gram-negative bacterial genomes. *Appl Environ Microbiol.* 1998;
782 64:2710–2715.
783 Derrien D, Marol C, Balesdent J. The dynamics of neutral sugars in the rhizosphere of wheat.
784 An approach by 13 C pulse-labelling and GC/C/IRMS. *Plant and Soil*. 2004; 267: 243-253.

785 DeShazer D, Brett PJ, Carlyon R, Woods DE. Mutagenesis of *Burkholderia pseudomallei*
786 with Tn5-OT182: isolation of motility mutants and molecular characterization of the flagellin
787 structural gene. *J Bacteriol.* 1997; 179:2116–2125.
788 Dilks K, Rose RW, Hartmann E, Pohlschroder M. Prokaryotic utilization of the Twin-
789 Arginine Translocation pathway: a genomic survey. *J Bacteriol.* 2003; 185:1478-1483.
790 Driessen AJ, Wickner W. Proton transfer is rate-limiting for translocation of precursor
791 proteins by the Escherichia coli translocase. *Proc Natl Acad Sci*. 1991; 88:2471-2475.
792 Ebert BE, Kurth F, Grund M, Blank LM, *et al.* Response of *Pseudomonas putida* KT2440 to
793 increased NADH and ATP demand. *Appl Environ Microbiol*. 2011; 77:6597-6605.
794 El-Gebali S, Mistry J, Bateman A, Eddy SR, *et al.* The Pfam protein families database in
795 *Nucleic Acids Res.* 2019; 47:D427–D432.
796 Ferri S, Kojima K, Sode K. Review of glucose oxidases and glucose dehydrogenases: A
797 bird's eye view of glucose sensing enzymes. *J Diabetes Sci Technol*. 2011;5:1068–1076.
798 Gadd GM. Geomycology: biogeochemical transformations of rocks, minerals, metals and
799 radionuclides by fungi, bioweathering and bioremediation. *Mycol Res.* 2007; 111:3–49.
800 Goldstein AH. Recent progress in understanding the molecular genetics and biochemistry of
801 calcium phosphate solubilization by Gram negative bacteria. *Biol Agric Hortic.* 1995;12:185–
802 193.
803 Goldstein A, Lester T, Brown J. Research on the metabolic engineering of the direct oxidation
804 pathway for extraction of phosphate from ore has generated preliminary evidence for PQQ
805 biosynthesis in *Escherichia coli* as well as a possible role for the highly conserved region of
806 quinoprotein dehydrogenases. Biochim Biophys Acta BBA - *Proteins Proteomics*. 2003;
807 1647:266–271.

808 Gouy M, Guindon S, Gascuel O. SeaView Version 4: A Multiplatform Graphical User
809 Interface for Sequence Alignment and Phylogenetic Tree Building. *Mol Biol Evol.* 2010;
810 27:221–224.
811 Grayston SJ, Campbell CD. Functional biodiversity of microbial communities in the
812 rhizospheres of hybrid larch (*Larix eurolepis*) and Sitka spruce (*Picea sitchensis*). Tree
813 Physiol. 1996;16:1031-1038.
814 Hinsinger P, Plassard C, Tang C, Jaillard B. Origins of root-mediated pH changes in the
815 rhizosphere and their responses to environmental constraints: A review. *Plant Soil* 2003;
816 248:43–59.
817 Jolivet C, Angers DA, Chantigny MH, Andreux F, Arrouays D. Carbohydrate dynamics in
818 particle-size fractions of sandy spodosols following forest conversion to maize cropping. Soil
819 Biology and Biochemistry. 2006; 38:2834-2842.
820 Jongmans AG, van Breemen N, Lundström U, van Hees PAW, *et al.* Rock-eating fungi.
821 Nature 1997; 389:682–683.
822 Kawai S, Goda-Tsutsumi M, Yakushi T, Kano K, *et al.* Heterologous overexpression and
823 characterization of a flavoprotein-cytochrome c complex fructose dehydrogenase of
824 *Gluconobacter japonicus* NBRC3260. *Appl Environ Microbiol.* 2013; 79:1654–1660.
825 Kovacs N. Identification of *Pseudomonas pyocyanea* by the oxidase reaction. Nature 1956;
826 178:703–703.
827 Kovach ME, Elzer PH, Steven Hill D, Robertson GT, *et al.* Four new derivatives of the
828 broad-host-range cloning vector pBBR1MCS, carrying different antibiotic-resistance
829 cassettes. Gene 1995; 166:175–176.
830 Koele N, Turpault M-P, Hildebrand EE, Uroz S, *et al.* Interactions between mycorrhizal fungi
831 and mycorrhizosphere bacteria during mineral weathering: Budget analysis and bacterial
832 quantification. *Soil Biol Biochem*. 2009; 41:1935–1942.

833 Kranz RG, Richard-Fogal C, Taylor J-S, Frawley ER. Cytochrome c biogenesis: mechanisms
834 for covalent modifications and trafficking of heme and for heme-iron redox control.
835 *Microbiol Mol Biol Rev.* 2009; 73:510–528.
836 Landeweert R, Hoffland E, Finlay RD, Kuyper TW, *et al.* Linking plants to rocks:
837 ectomycorrhizal fungi mobilize nutrients from minerals. *Trends Ecol Evol.* 2001; 16:248–254.
838 Lepleux C, Turpault MP, Oger P, Frey-Klett P, Uroz S. 2012. Correlation of the abundance of
839 betaproteobacteria on mineral surfaces with mineral weathering in forest soils. *Appl Environ*
840 *Microbiol*. 2012; 78:7114-7119.
841 Leveau JHJ, Uroz S, de Boer W. The bacterial genus *Collimonas* : mycophagy, weathering
842 and other adaptive solutions to life in oligotrophic soil environments. *Environ Microbiol*.
843 2010; 12:281–292.
844 Lidbury IDEA, Murphy ARJ, Scanlan DJ, Bending GD, *et al.* Comparative genomic,
845 proteomic and exoproteomic analyses of three *Pseudomonas* strains reveals novel insights
846 into the phosphorus scavenging capabilities of soil bacteria: Comparative genomic, proteomic
847 and exoproteomic analyses of three Pseudomonas strains. *Environ Microbiol*. 2016;18:3535–
848 3549.
849 Liu ST, Lee LY, Tai CY, Hung CH, *et al.* Cloning of an *Erwinia herbicola* gene necessary for
850 gluconic acid production and enhanced mineral phosphate solubilization in *Escherichia coli*
851 HB101: nucleotide sequence and probable involvement in biosynthesis of the coenzyme
852 pyrroloquinoline quinone. *J Bacteriol.* 1992;174:5814–5819.
853 Martin, F., D. Canet, Marchal JP. *In vivo* abundance 13C NMR studies of the carbohydrate
854 storage in ectomycorrhizal fungi. *Physiol Veg*. 1984; 22:733–743.
855 Matsushita, K., Ameyama, M. [24] d-Glucose dehydrogenase from *Pseudomonas fluorescens*,
856 membrane-bound. In Methods in enzymology (Vol. 89, pp. 149-154). 1982; Academic Press.

857 Medeiros PM, Fernandes MF, Dick RP, Simoneit BR. Seasonal variations in sugar contents
858 and microbial community in a ryegrass soil. *Chemosphere*. 2006; 65:832-839.
859 Mela F, Fritsche K, de Boer W, van den Berg M *et al.* Comparative genomics of bacteria
860 from the genus *Collimonas*: linking (dis)similarities in gene content to phenotypic variation
861 and conservation. *Environ Microbiol Rep*. 2012; 4:424–432.
862 Palmer T, Berks BC. The twin-arginine translocation (Tat) protein export pathway. *Nat Rev*
863 *Microbiol.* 2012 10:483–496.
864 Picard L, Oger, P, Turpault, M-P, Uroz, S. Draft genome of *Collimonas pratensis* strain
865 PMB3(1), an effective mineral weathering and chitin hydrolyzing bacterial strain. Microbial
866 Genom. Res. DOI: 10.1128/MRA.00601-20
867 Pospiech AA versatile quick-prep of genomic DNA from Gram-positive bacteria. *Trends*
868 *Genet* . 199511:217–218.
869 Puente ME, Bashan Y, Li CY, Lebsky VK. Microbial populations and activities in the
870 rhizoplane of rock-weathering desert plants. II. Growth promotion of cactus seedlings. *Plant*
871 *Biol*. 2004; 6:643–649.
872 Ranger J, Turpault M-P. Input–output nutrient budgets as a diagnostic tool for sustainable
873 forest management. *For Ecol Manag.* 1999; 122:139–154.
874 Rodríguez H, Fraga R. Phosphate solubilizing bacteria and their role in plant growth
875 promotion. *Biotechnol Adv* . 1999; 17:319–339.
876 Saichana I, Moonmangmee D, Adachi O, Matsushita K, *et al.* Screening of thermotolerant
877 *Gluconobacter* strains for production of 5-Keto-D-gluconic acid and disruption of Flavin
878 Adenine Dinucleotide-containing D-gluconate dehydrogenase. *Appl Environ Microbiol.* 2009;
879 75:4240–4247.
880 Sasnow SS, Wei H, Aristilde L. Bypasses in intracellular glucose metabolism in iron-limited
881 Pseudomonas putida. MicrobiologyOpen 2016; 5:3–20.

882 Shiota M, Yamazaki T, Yoshimatsu K, Kojima K, *et al.* An Fe–S cluster in the conserved
883 Cys-rich region in the catalytic subunit of FAD-dependent dehydrogenase complexes.
884 Bioelectrochem. 2016; 112:178–183.
885 Sützl L, Foley G, Gillam EMJ, Bodén M, *et al.* The GMC superfamily of oxidoreductases
886 revisited: analysis and evolution of fungal GMC oxidoreductases. Biotechnol Biofuels 2019;
887 12:1–18.
888 Toyama H, Furuya N, Saichana I, Ano Y, *et al.* Membrane-bound, 2-keto-D-gluconate-
889 yielding D-gluconate dehydrogenase from Gluconobacter dioxyacetonicus IFO 3271:
890 molecular properties and gene disruption. *Appl Environ Microbiol.* 2007; 73:6551–6556.
891 Toyama H, Soemphol W, Moonmangmee D, Adachi O, *et al.* Molecular properties of
892 membrane-bound FAD-containing D-Sorbitol dehydrogenase from thermotolerant
893 *Gluconobacter frateurii* isolated from Thailand. *Biosci Biotechnol Biochem.* 2005; 69:1120–
894 1129.
895 Turpault MP, Nys C, Calvaruso C. Rhizosphere impact on the dissolution of test minerals in a
896 forest ecosystem. Geoderma. 2009; 153:147–154.
897 Udovičić M, Sievers M, Zhang D-C, Margesin R, *et al. Glaciimonas alpina* sp. nov. isolated
898 from alpine glaciers and reclassification of Glaciimonas immobilis Cr9-12 as the type strain
899 of *Glaciimonas alpina* sp. nov. *Int J Syst Evol Microbiol*. 2015; 65:1779–1785.
900 Uroz S, Calvaruso C, Turpault MP, Pierrat JC, *et al.* Effect of the mycorrhizosphere on the
901 genotypic and metabolic diversity of the bacterial communities involved in mineral
902 weathering in a forest soil. *Appl Environ Microbiol.* 2007;73:3019–3027.
903 Uroz S, Calvaruso C, Turpault M-P, Frey-Klett P. Mineral weathering by bacteria: ecology,
904 actors and mechanisms. *Trends Microbiol.* 2009; 17:378–387.

Uroz S, Calvaruso C, Turpault M-P, Sarniguet A, *et al.* 2009b. Efficient mineral weathering is a distinctive functional trait of the bacterial genus Collimonas. *Soil Biol Biochem.* 2009; 41:2178–2186.

Uroz S, Turpault M-P, Van Scholl L, Palin B, *et al.* Long term impact of mineral amendment on the distribution of the mineral weathering associated bacterial communities from the beech *Scleroderma citrinum* ectomycorrhizosphere. *Soil Biol Biochem.* 2011; 43:2275–2282.

Uroz S, Picard L, Turpault M-P, Auer L, *et al.* Dual transcriptomic and proteomic analyses of the early stage of interaction between *Caballeronia mineralivorans* PML1(12) and mineral. In press. Environmental Microbiol. doi:10.1111/1462-2920.15159

Vallenet D, Engelen S, Mornico D, Cruveiller S, MicroScope: a platform for microbial genome annotation and comparative genomics. Database 2009.

Wagh J, Shah S, Bhandari P, Archana G,*et al.* Heterologous expression of pyrroloquinoline quinone (pqq) gene cluster confers mineral phosphate solubilization ability to *Herbaspirillum seropedicae* Z67. Appl Microbiol Biotechnol. 2014; 98:5117–5129.

Wang Y-L, Sun L-J, Xian C-M, Kou F-L, *et al.* Interactions between biotite and the mineral-weathering bacterium *Pseudomonas azotoformans* F77. *Appl Environ Microbiol.* 2020 86:e02568-19.

Yamaoka H, Yamashita Y, Ferri S, Sode K. Site directed mutagenesis studies of FAD-dependent glucose dehydrogenase catalytic subunit of *Burkholderia cepacia*. *Biotechnol Lett.* 2008; 30:1967–1972.

Zámocký M, Hallberg M, Ludwig R, Divne C, *et al.* Ancestral gene fusion in cellobiose dehydrogenases reflects a specific evolution of GMC oxidoreductases in Fungi. Gene 2004; 338:1–14.

928 Zhang, Z., Huang, J., He, L., Sheng, X. Distinct weathering ability and populations of
929 culturable mineral-weathering bacteria in the rhizosphere and bulk soils of Morus alba.
930 Geomicrobiology J. 2016; 33:39-45.

931
932
933
934
935
936
937
938
939
940
941
942
943
944
945
946
947
948
949
950
951
952
953
954
955
956
957

FIGURE LEGENDS:

Figure 1: Thin layer chromatography analysis of gluconic acid production by the wild type strain PMB3(1) of *Collimonas pratensis*

A volume of 8 µl of supernatant of ABm culture was spotted on the TLC. Cultures were done in ABm medium supplemented with 10 g/l of glucose inoculated or not with the WT strain PMB3(1). The supernatant was recovered after 4 days of incubation at 25°C. A volume of 4 µl of standards was spotted on the TLC. Standards correspond to 100 mM solutions of glucose, gluconate, 2KGA and 5KGA. After revelation, glucose appeared in dark blue spots, gluconate in pink, 2KGA in brown and 5KGA in dark purple spot. The pink arrow indicates the pink spot of the gluconate standard.

Figure 2: Biotite dissolution assay by the WT and mutant strains

(A) Measure of iron released from biotite after 7 days of incubation at 25°C in BHm supplemented with (2 g/l) glucose ; **(B)** Measure of pH measurement with bromocresol green. The control treatment termed 'Biotite' corresponds to the non-inoculated treatment. It allows the measurement of the spontaneous release of iron from biotite in the medium in our experimental conditions. The second control termed 'medium' corresponds to the non-inoculated medium without biotite. Each value is the mean of three independent replicates ± the standard error of the mean. Measures with different letters are significantly different according to an ANOVA test ($P<0.05$) ; **(C)** Individual mineral-weathering potentials (pH versus Fe released) of the WT strain and related MW mutants. White and grey squares correspond to the controls of the experiment (white, medium without biotite and non inoculated; grey, medium with biotite and non inoculated). The two curves indicate the

mineral-weathering effect of a complexing agent (citric acid) (dashed line) and a strong acid (hydrochloric acid) (solid line).

Figure 3: Genomic region of the plasposon insertion in the different mutants

For each mutant, the genes have been represented with large horizontal arrows and their length was scaled according to their nucleotidic size. The genes or group of genes directly impacted by the Tn5-OT182 insertion are filled with colour. The small black arrow indicates the location of the insertion of the Tn5-OT182 in the genome of PMB3(1) as identified by BlastN for the mutants 25(10F) **(A)**, 31(11B) **(B)**, 34(11H) **(C)** and 59(7B) **(D)**. Gene annotation is presented under each gene and the complete description is provided in Table 2 and in the supplementary Table S1, S2 and S3.

Figure 4: Growth test on WT, mutants and complemented mutants in LB broth

Growth monitoring of the wild type strain and of the mutants 25(10F), 31(11B) and 34(11H) complemented or not was done in LB medium over a period of 120 h. Growth was performed under orbital shaking and the measures correspond to absorbance measurement at λ600 nm. Each point is the mean of 3 independent replicates. For legibility reason, the standard error was not presented.

Figure 5: Acidification ability and growth on different carbon sources for the WT and mutants strains

The acidification (right axis) after 5 days of incubation at 25°C of the BHm medium with different carbon source (glucose, gluconate, 2keto gluconate and 5-keto gluconate) is presented by coloured circles according to the strain considered. The absorbance at 595 nm (left axis) representing the growth of the different strains is presented by coloured bars. The

non-inoculated medium was used as control. Each value is the mean of three independent replicates ± the standard error of the mean.

Figure 6: Molecular mechanisms of PQQ-independent GDH in mineral weathering process of *Collimonas pratensis* PMB3(1)

The hypothetical functional model presented in here was generated based on the data extracted in this study and from the literature. The GDH of the strain *Collimonas pratensis* PMB3(1) is composed of three subunits GdhS, GdhL and GdhC (blue). The GdhL subunit is able to bind the cofactor FAD (yellow) in the cytoplasm. The complex GdhS-GdhL is formed in the cytoplasm and then transported in the periplasm. This transfer is done through the Twin Arginine Translocation system (green), due to the presence of a TAT signal of the GdhS subunit. The functioning of the TAT system is based on the proton motive force. The cytochrome subunit (GdhC) is maturated by the ResABC system (orange) and translocated in the periplasm where it fixes heme. The GDH converts glucose in gluconate (GA) and protons (pink). Gluconate is then converted to 2-Keto-gluconate (2KGA) by the gluconate dehydrogenase (grey). The conversion of glucose to gluconic acid and then to 2KGA corresponds to the direct oxidative pathway (dotted red box). The 2KGA can go to the cytoplasm where it is then converted into 6-P-gluconate by a 2-keto gluconate kinase and a 2-keto gluconate 6-phosphate reductase prior to enter in the Pentose or the Entner-Doudoroff pathways. Both GA and 2KGA support the growth of strain PMB3(1). Protons produced by GDH activity lead to an acidification of the extracellular environment and permit the dissolution of minerals through acidolysis. The mineral weathering makes nutrients available to bacteria.

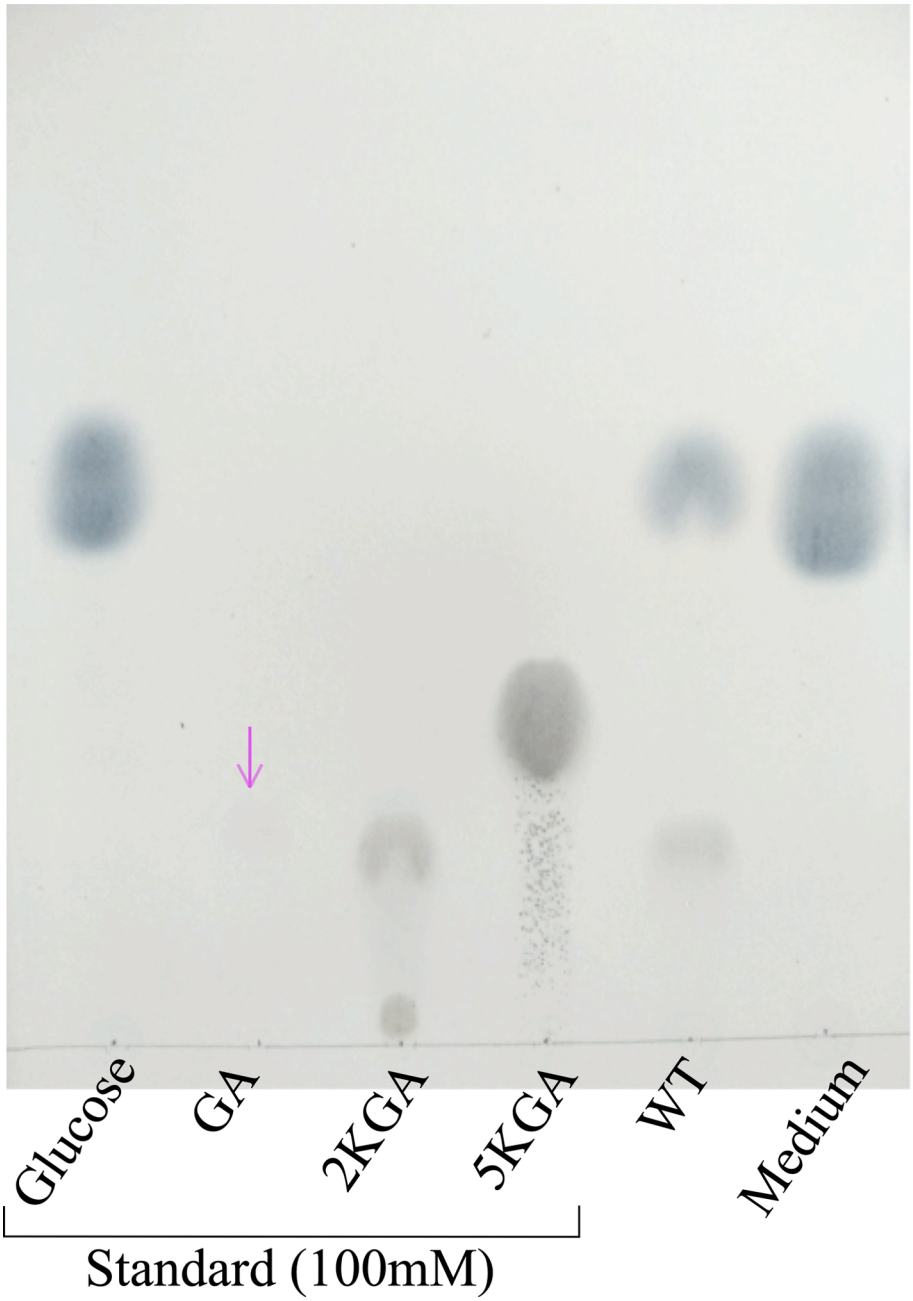
Glucose
GA
2KGA
5KGA
WT
Medium
Standard (100mM)

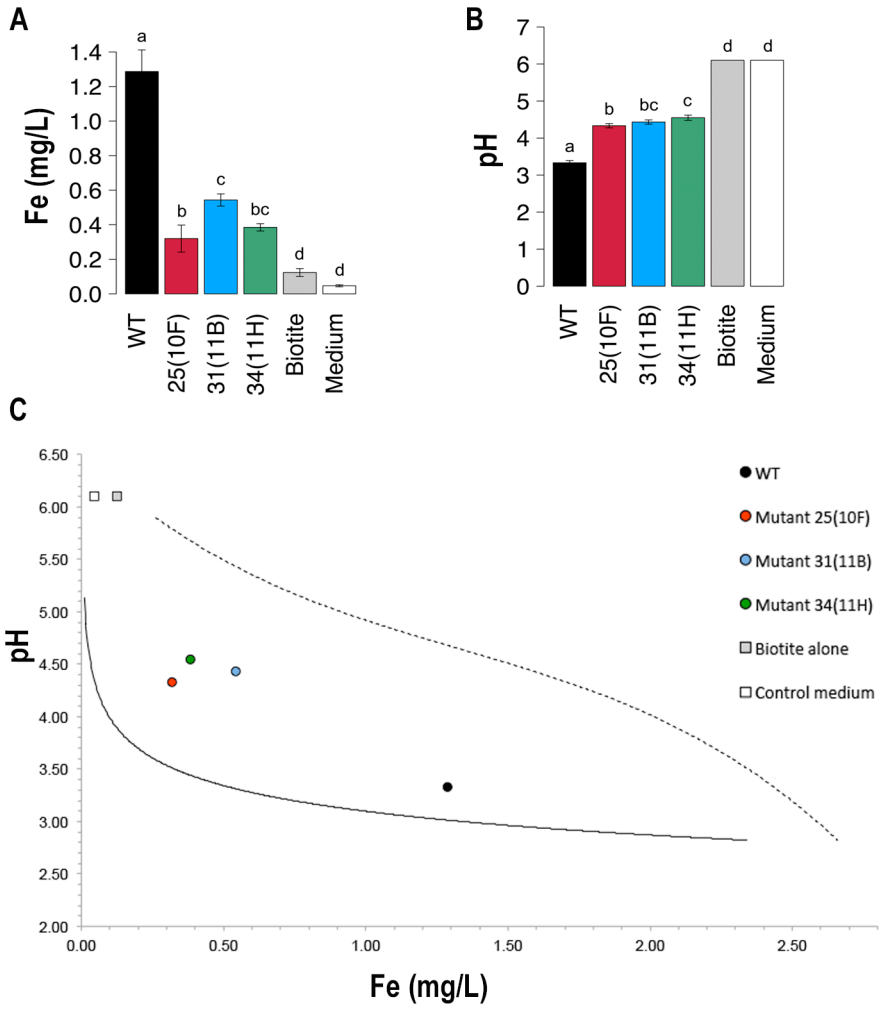
A
Fe (mg/L)
1.4
1.2
1.0
0.8
0.6
0.4
0.2
0.0
a
b
c
bc
d
d
WT
25(10F)
31(11B)
34(11H)
Biotite
Medium
B
pH
7
6
5
4
3
2
1
0
a
b
bc
c
d
d
WT
25(10F)
31(11B)
34(11H)
Biotite
Medium
C
pH
6.50
6.00
5.50
5.00
4.50
4.00
3.50
3.00
2.50
2.00
0.00
0.50
1.00
1.50
2.00
2.50
Fe (mg/L)
WT
Mutant 25(10F)
Mutant 31(11B)
Mutant 34(11H)
Biotite alone
Control medium

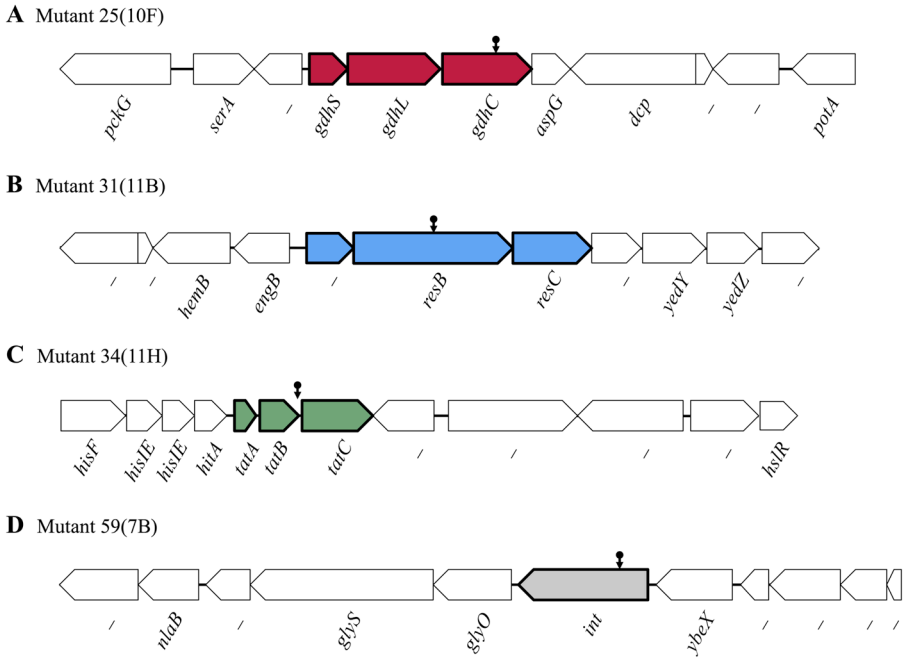
A Mutant 25(10F)
pckG
serA
gdhS
gdhL
gdhC
aspG
dcp
potA
B Mutant 31(11B)
hemB
engB
resB
resC
yedY
yedZ
C Mutant 34(11H)
hisF
hisIE
hisIE
hitA
tatA
tatB
tatC
hslR
D Mutant 59(7B)
nlaB
glyS
glyO
int
ybeX

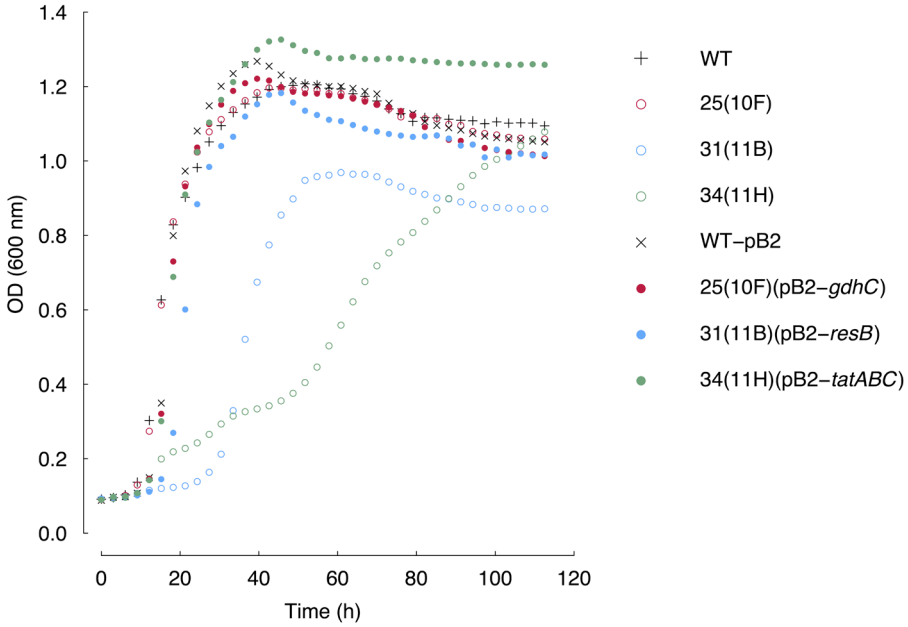
OD (600 nm)
Time (h)
0.0
0.2
0.4
0.6
0.8
1.0
1.2
1.4
0
20
40
60
80
100
120
WT
25(10F)
31(11B)
34(11H)
WT–pB2
25(10F)(pB2–gdhC)
31(11B)(pB2–resB)
34(11H)(pB2–tatABC)

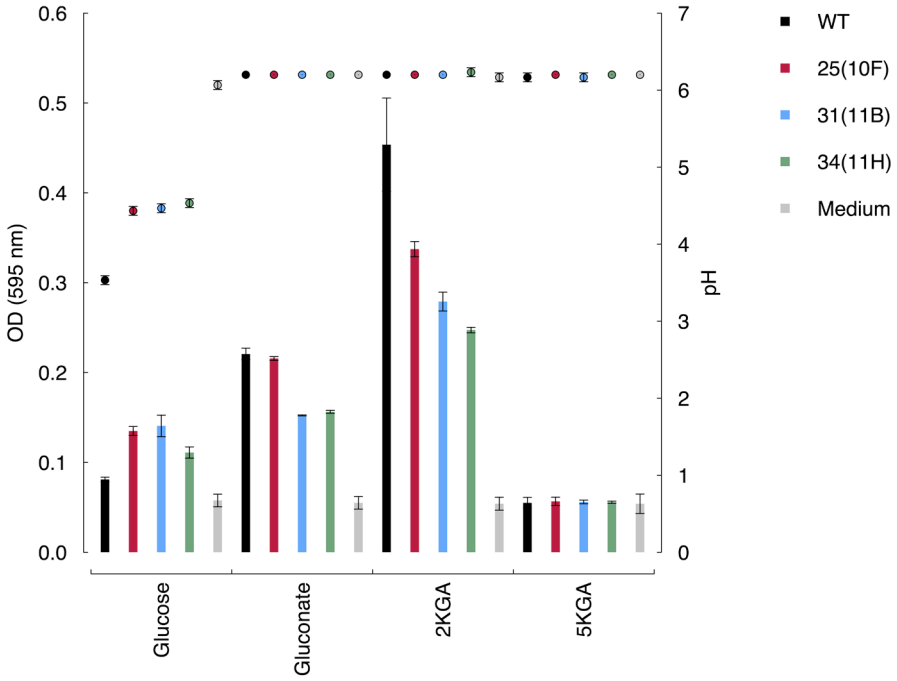
0.6
0.5
0.4
0.3
0.2
0.1
0.0
OD (595 nm)
7
6
5
4
3
2
1
0
pH
WT
25(10F)
31(11B)
34(11H)
Medium
Glucose
Gluconate
2KGA
5KGA

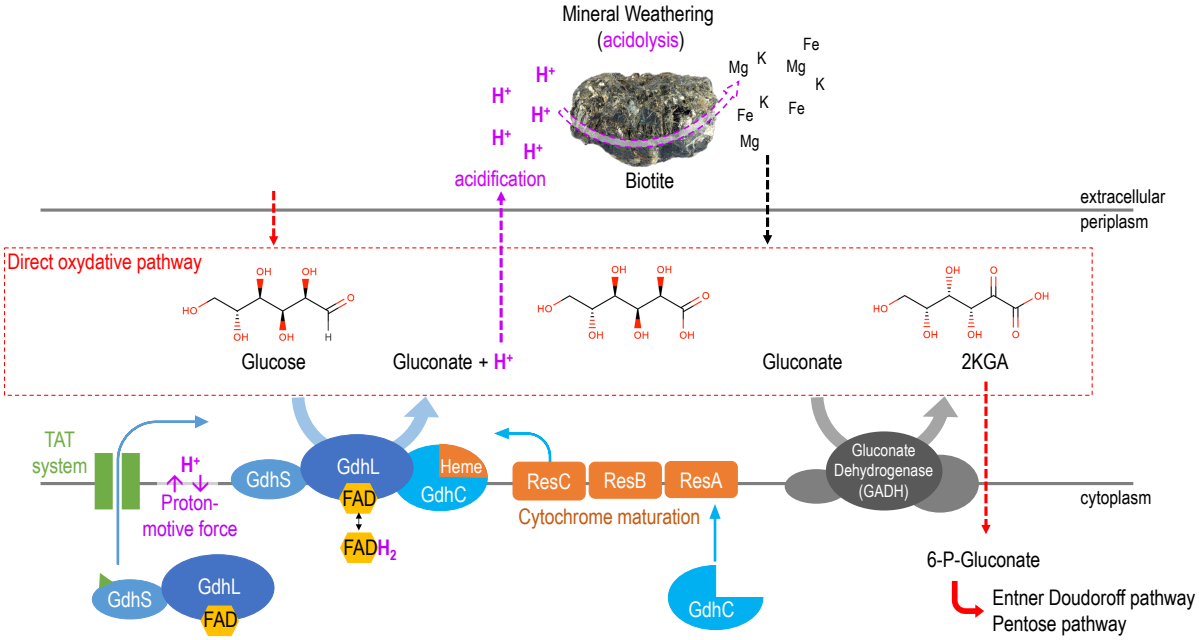

SUPLEMENTAL MATERIAL

Identification of a novel type of glucose dehydrogenase involved in the mineral weathering ability of *Collimonas pratensis* strain PMB3(1)

Picard, L.[1,2], Turpault, M-P. [2], Oger, P.M.[3], Uroz, S. [1,2#]

1133

1134

1135 **Table S1 : Description of the genomic region of the plasposon insertion in mutant 31(11B)**

Accession number	Putative function	Gene annotation	Length (nt)	BLASTP (% Id against NCBI)		
NKI71669.1	Mg2+ transporter protein, cora-like protein	_	1149	93%	Magnesium transporter cora family protein [WP_098495086.1]	Collimonas sp. PA-H2
NI*	Protein of unknown function	_	195	97%	Hypothetical protein cpter291_0433 [AMP12718.1]	Collimonas pratensis
NKI71670.1	Delta-aminolevulinic acid dehydratase	hemB	1068	99%	Porphobilinogen synthase [PFH10198.1]	Collimonas sp. PA-H2
NKI71671.1	Putative GTP-binding protein engb	engB	732	95%	Yiha family ribosome biogenesis GTP-binding protein [WP_098495089.1]	Collimonas sp. PA-H2
NKI71672.1	Cytochrome c4	_	666	99%	Cytochrome c4 [WP_098495090.1]	Collimonas sp. PA-H2
NKI71673.1	**Cytochrome c-type biogenesis protein Ccs1/ResB**	**resB**	**2160**	**94%**	**Cytochrome c biogenesis protein resb [WP_098495091.1]**	**Collimonas sp. PA-H2**
NKI71674.1	Cytochrome c-type biogenesis protein ccsa/resc	resC	1146	99%	C-type cytochrome biogenesis protein ccsb [WP_098497480.1]	Collimonas sp. PA-H2

NKI71675.1	Putative phosphatase yieh	_	684	92%	HAD family hydrolase [WP_098495092.1]	Collimonas sp. PA-H2
NKI71676.1	Exported heme-molybdoenzyme molybdopterin-containing subunit yedy; TAT export	yedY	981	94%	Protein-methionine-sulfoxide reductase catalytic subunit msrp [WP_098495093.1]	Collimonas sp. PA-H2
NKI71677.1	Sulfoxide reductase heme-binding subunit yedz	yedZ	669	89%	Sulfoxide reductase heme-binding subunit yedz [WP_098495094.1]	Collimonas sp. PA-H2
NKI71678.1	Conserved exported protein of unknown function	_	825	87%	Transporter [WP_092414082.1]	Collimonas sp. OK307

1136 * Some of the proteins listed have not been identified (NI) according to the prediction tools used by NCBI, but were predicted in the MICROSCOPE platform.

1137

1138

1139 **Table S2 : Description of the genomic region of the plasposon insertion in mutant 34(11H)**

Accession number	Putative function	Gene annotation	Length (nt)	BLASTP (%Id against NCBI)		
NKI71753.1	Imidazole glycerol phosphate synthase, catalytic subunit with hish	hisF	765	99%	Imidazole glycerol phosphate synthase subunit hisf [WP_092356093.1]	Collimonas sp. OK242
NKI71754.1	Fragment of bifunctional protein [Includes: phosphoribosyl-AMP cyclohydrolase; phosphoribosyl-ATP pyrophosphatase] (part 1)	hisIE	396	97%	Phosphoribosyl-AMP cyclohydrolase [WP_092434873.1]	Collimonas sp. OK607
NKI71755.1	Fragment of bifunctional protein [Includes: phosphoribosyl-AMP cyclohydrolase; phosphoribosyl-ATP pyrophosphatase] (part 2)	hisIE	378	94%	Phosphoribosyl-ATP diphosphatase [WP_098495230.1]	Collimonas sp. PA-H2
NKI71756.1	Protein hita	hitA	372	93%	Histidine triad nucleotide-binding protein [WP_098495231.1]	Collimonas sp. PA-H2
NKI71757.1	Sec-independent protein translocase protein	tatA	231	95%	Twin-arginine translocation protein	Collimonas fungivorans

	tata				tata [AEK60361.1]	Ter331
NKI71758.1	Sec-independent protein translocase protein tatb	tatB	495	93%	Sec-independent protein translocase subunit tatb [WP_098495232.1]	Collimonas sp. PA-H2
NKI71759.1	**Tatabce protein translocation system subunit**	**tatC**	**768**	**95%**	**Twin-arginine translocase subunit tatc [WP_098495233.1]**	**Collimonas sp. PA-H2**
NKI71760.1	Conserved protein of unknown function	_	690	97%	DUF2461 domain-containing protein [WP_098495234.1]	Collimonas sp. PA-H2
NKI71761.1	Emrb/qaca subfamily drug resistance transporter	_	1452	94%	DHA2 family efflux MFS transporter permease subunit [WP_098495235.1]	Collimonas sp. PA-H2
NKI71762.1	Putative htra-like serine protease	_	1167	98%	Do family serine endopeptidase [WP_098495236.1]	Collimonas sp. PA-H2
NKI71763.1	Putative GTP cyclohydrolase 1 type 2	_	768	93%	Dinuclear metal center ybgi/SA1388 family protein [PFH10368.1]	Collimonas sp. PA-H2
NKI71764.1	Heat shock protein 15 homolog	hslR	387	96%	RNA-binding S4 domain-containing protein [WP_098495238.1]	Collimonas sp. PA-H2

1140

1141

1142 **Table S3 : Description of the genomic region of the plasposon insertion in mutant 59(7B)**

Accession number	Putative function	Gene annotation	Length (nt)	Blastp (%id against ncbi)	
NKI72634.1	Zinc metalloprotease	_	984	93%	Hypothetical protein BCF11_1207 [PFH08832.1]	Collimonas sp. PA-H2
NKI72635.1	1-acyl-sn-glycerol-3-phosphate acyltransferase	nlaB	744	98%	1-acyl-sn-glycerol-3-phosphate acyltransferase [WP_098493940.1]	Collimonas sp. PA-H2
NKI72636.1	D-glycero-beta-D-manno-heptose-1,7-bisphosphate 7-phosphatase	_	558	97%	D-glycero-beta-D-manno-heptose 1,7-bisphosphate 7-phosphatase [WP_098493939.1]	Collimonas sp. PA-H2
NKI72637.1	Glycine trna synthetase, beta subunit	glyS	2133	96%	Glycine--trna ligase subunit beta [WP_098493938.1]	Collimonas sp. PA-H2
NKI72638.1	Glycyl-trna synthetase, alpha chain	glyQ	981	99%	Glycine--trna ligase subunit alpha [WP_098493937.1]	Collimonas sp. PA-H2
NKI72639.1	**Apolipoprotein N-acyltransferase**	**lnt**	**1554**	**92%**	**Apolipoprotein N-acyltransferase**	**Collimonas sp. PA-**

					[WP_098493936.1]	**H2**
NKI72640.1	Putative protein involved in divalent ion export	ybeX	882	99%	CBS domain-containing protein [WP_098493935.1]	Collimonas sp. PA-H2
NKI72641.1	Conserved exported protein of unknown function	_	267	83%	Pentapeptide MXKDX repeat protein [WP_098497346.1]	Collimonas sp. PA-H2
NKI72642.1	Oxidoreductase, molybdopterin binding protein	_	780	97%	Molybdopterin-dependent oxidoreductase [WP_098493934.1]	Collimonas sp. PA-H2
NKI72643.1	Thiosulfate reductase cytochrome B subunit (Membrane anchoring protein)	_	615	94%	Cytochrome b/b6 domain-containing protein [WP_098493933.1]	Collimonas sp. PA-H2
NI*	Protein of unknown function	_	114	97%	Hypothetical protein cpter91_4422 [AMP06731.1]	Collimonas pratensis

* Some of the proteins listed have not been identified (NI) according to the prediction tools used by NCBI, but were predicted in the MICROSCOPE platform.

Table S4: List of proteins carrying a TAT-signal in the strain *Collimonas pratensis* PMB3(1)

The COG class of each protein is indicated with one-letter abbreviation as followed: P, inorganic ion transport and metabolism; Q, secondary metabolites biosynthesis, transport and catabolism; C, energy production and conversion; E, amino acid metabolism and transport; F, nucleotide metabolism and transport; G, carbohydrate metabolism and transport; H, coenzyme and metabolism; J, translation, ribosomal structure and biogenesis; K, transcription; L, replication, recombination and repair; M, cell wall, membrane, envelope biogenesis; N, cell motility; O, posttranslational modification, protein turnover, chaperones; S, function unknown; U, intracellular trafficking, secretion, and vesicular transport; W, extracellular structures. The bold rows indicated the proteins mentioned in the text and could be involved in MW. Some of the proteins listed have not been identified (NI) according to the prediction tools used by NCBI, but were predicted in the MICROSCOPE platform.

Accession number (MAGE)	Gene annotation	Putative function	COG class
NKI68675.1	yagR	Aerobic-type carbon monoxide dehydrogenase, large subunit	C
NKI69300.1	iorB	Isoquinoline 1-oxidoreductase beta subunit	C
NKI69617.1	soxH	putative cytochrome C oxidase polypeptide II oxidoreductase protein	C
NKI71676.1	yedY	exported heme-molybdoenzyme molybdopterin-containing subunit YedY; TAT export	C
NKI72252.1	mqo	malate dehydrogenase, FAD	C
NKI72324.1	FAD	FMN-dependent dehydrogenase	C

NKI67910.1		exported protein of unknown function	C
NKI69616.1		conserved protein of unknown function	C
NKI68636.1		putative branched-chain amino acid transport protein (ABC superfamily, peri_bind)	E
NKI68806.1		ABC transporter substrate-binding protein	E
NKI69719.1	aguA	putative agmatine deiminase	E
NKI69739.1	ggtA	Gamma-glutamyltranspeptidase	E
NKI72278.1		Monoamine oxidase	E
NKI71314.1		conserved protein of unknown function	E
NKI68557.1	rihA	Pyrimidine-specific ribonucleoside hydrolase RihA	F
NKI71053.1		putative nucleoside hydrolase	F
NKI67981.1	ykgB	putative hemagglutinin-like protein	G
NKI68770.1	bga	Beta-galactosidase	G
NKI69257.1	ytfQ	putative sugar transporter subunit: periplasmic-binding component of ABC superfamily	G
NKI68420.1		conserved membrane protein of unknown function	G
NKI69773.1		conserved exported protein of unknown function	G
NKI72549.1		conserved exported protein of unknown function	H
NKI71161.1		Amidase, Asp-tRNAAsn/Glu-tRNAGln amidotransferase A subunit	J
NKI71645.1	rplP	50S ribosomal protein L16	J
NI		protein of unknown function	J

NKI68641.1		LysR family transcriptional regulator	K
NKI72806.1		transposase	L
NKI68262.1	plcN	Non-hemolytic phospholipase C	M
NKI68666.1	mrcA	Penicillin-binding protein 1A	M
NKI69363.1	acpA	Acid phosphatase	M
NKI69405.1	plcN	Non-hemolytic phospholipase C	M
NKI71095.1	plcN	Non-hemolytic phospholipase C	M
NKI72507.1	amiC	N-acetylmuramoyl-L-alanine amidase	M
NKI68496.1		putative Peptide-N(4)-(N-acetyl-beta-glucosaminyl)asparagine amidase	N
NKI69248.1	ppiA	peptidyl-prolyl cis-trans isomerase A (rotamase A)	O
NKI69912.1	msrB	Methionine sulfoxide reductase	O
NKI72023.1		CcsA-like protein	O
NKI72219.1	lifO	Lipase chaperone	O
NKI72562.1		Methionine-R-sulfoxide reductase	O
NKI70121.1	mdoD	glucan biosynthesis protein, periplasmic	P
NKI71510.1	**phoD**	**Alkaline phosphatase**	P
NKI72113.1	nasF	Nitrate ABC transporter, nitrate-binding protein	P
NKI72201.1		ABC-type nitrate/sulfonate	P
NKI72274.1	Nitrate	sulfonate	P

NKI72605.1		**Alkaline phosphatase**	P
NKI72716.1	metQ	DL-methionine transporter subunit ; periplasmic-binding component of ABC superfamily	P
NKI67804.1	ysgA	putative hydrolase	Q
NKI68502.1		putative multicopper oxidase	Q
NI		protein of unknown function	Q
NKI71458.1		conserved exported protein of unknown function	Q
NKI72652.1		Type 4 fimbrial biogenesis protein PilY1	U
NKI72179.1		exported protein of unknown function	U
NKI70646.1		YadA-like protein	W
NKI68516.1	ars	Hydrolase	S
NKI68701.1		putative transmembrane protein	S
NKI68877.1		Sulfite dehydrogenase (Cytochrome) subunit SorA apoprotein	S
NKI69325.1	yvnB	LPXTG-motif cell wall anchor domain protein	S
NKI70794.1	**gdhS**	**Sorbitol/Glucose/2-Keto-D-gluconate dehydrogenase, membrane-bound, gamma subunit**	S
NKI71018.1		Phosphoserine phosphatase	S
NKI71108.1		putative secreted protein	S
NKI71438.1		Lipoprotein	S
NKI71603.1	ophA	ABC peptide	S
NKI68405.1		conserved exported protein of unknown function	S

NKI68510.1	conserved exported protein of unknown function	S
NKI68544.1	conserved protein of unknown function	S
NKI68550.1	protein of unknown function	S
NKI69712.1	conserved protein of unknown function	S
NKI70227.1	conserved protein of unknown function	S
NKI71034.1	conserved exported protein of unknown function	S
NKI71518.1	conserved exported protein of unknown function	S
NKI71778.1	exported protein of unknown function	S
NKI71790.1	conserved exported protein of unknown function	S
NI	protein of unknown function	S
NI	protein of unknown function	S

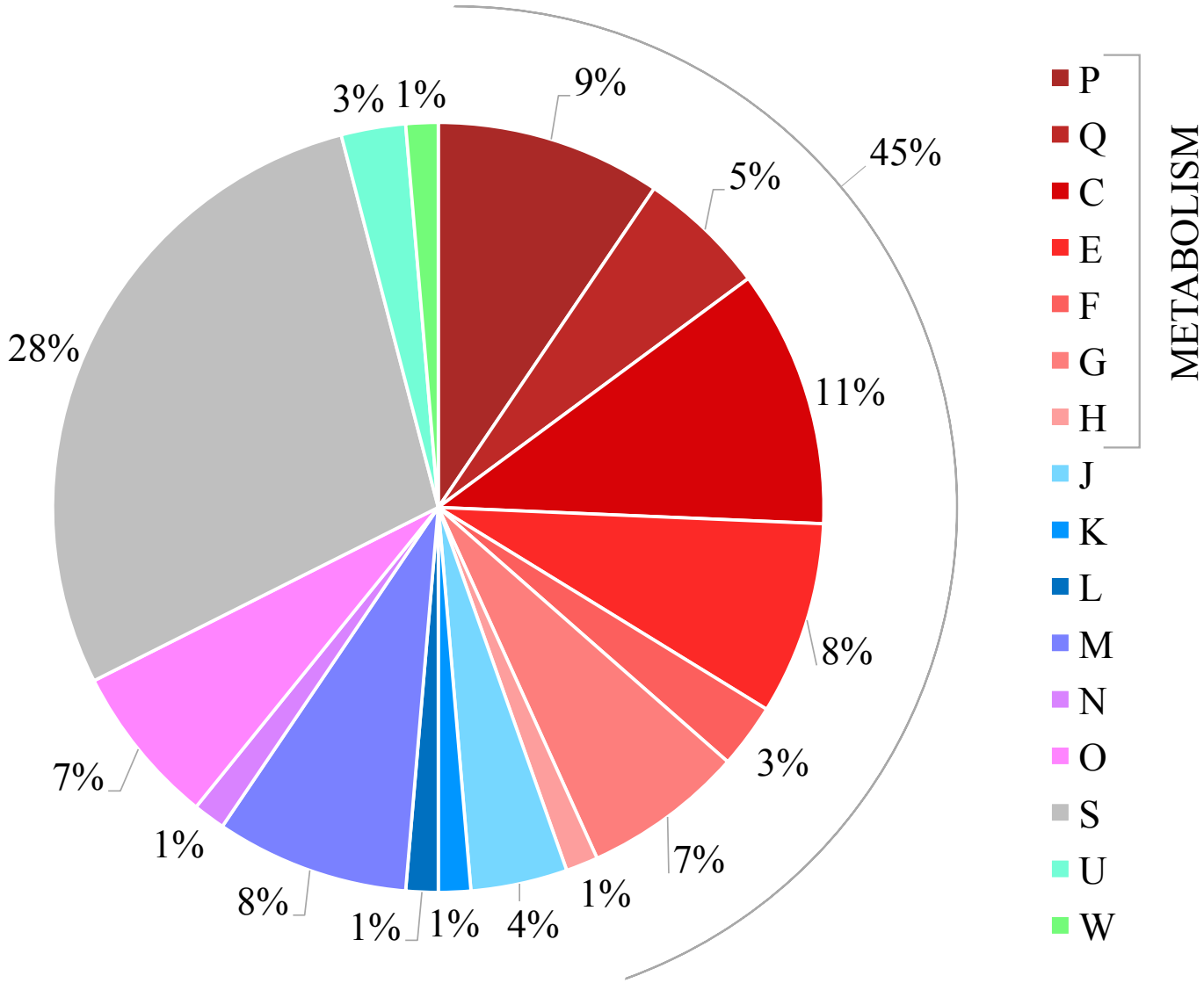

Figure S1 : COG class distribution of the TAT-proteins

The proteins highlighted in red colors light to dark are those involved in metabolism, which encompass ca. 45 % of the total TAT-proteins.

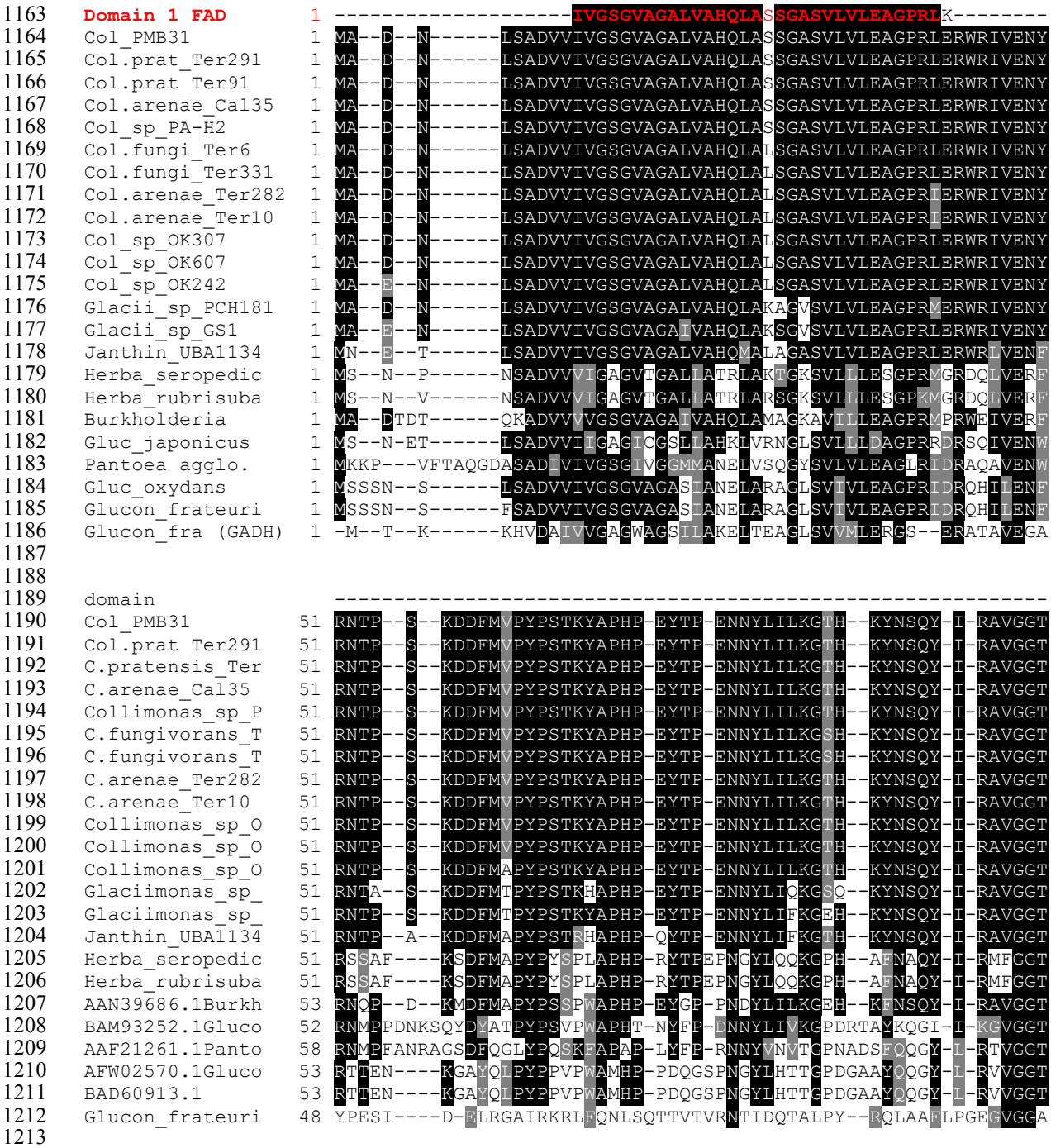
Domain 1 FAD
Col_PMB31
Col.prat_Ter291
Col.prat_Ter91
Col.arenae_Cal35
Col_sp_PA-H2
Col.fungi_Ter6
Col.fungi_Ter331
Col.arenae_Ter282
Col.arenae_Ter10
Col_sp_OK307
Col_sp_OK607
Col_sp_OK242
Glacii_sp_PCH181
Glacii_sp_GS1
Janthin_UBA1134
Herba_seropedic
Herba_rubrisuba
Burkholderia
Gluc_japonicus
Pantoea agglo.
Gluc_oxydans
Glucon_frateuri
Glucon_fra (GADH)
domain
Col_PMB31
Col.prat_Ter291
C.pratensis_Ter
C.arenae_Cal35
Collimonas_sp_P
C.fungivorans_T
C.fungivorans_T
C.arenae_Ter282
C.arenae_Ter10
Collimonas_sp_O
Collimonas_sp_O
Collimonas_sp_O
Glaciimonas_sp_
Glaciimonas_sp_
Janthin_UBA1134
Herba_seropedic
Herba_rubrisuba
AAN39686.1Burkh
BAM93252.1Gluco
AAF21261.1Panto
AFW02570.1Gluco
BAD60913.1
Glucon_frateuri

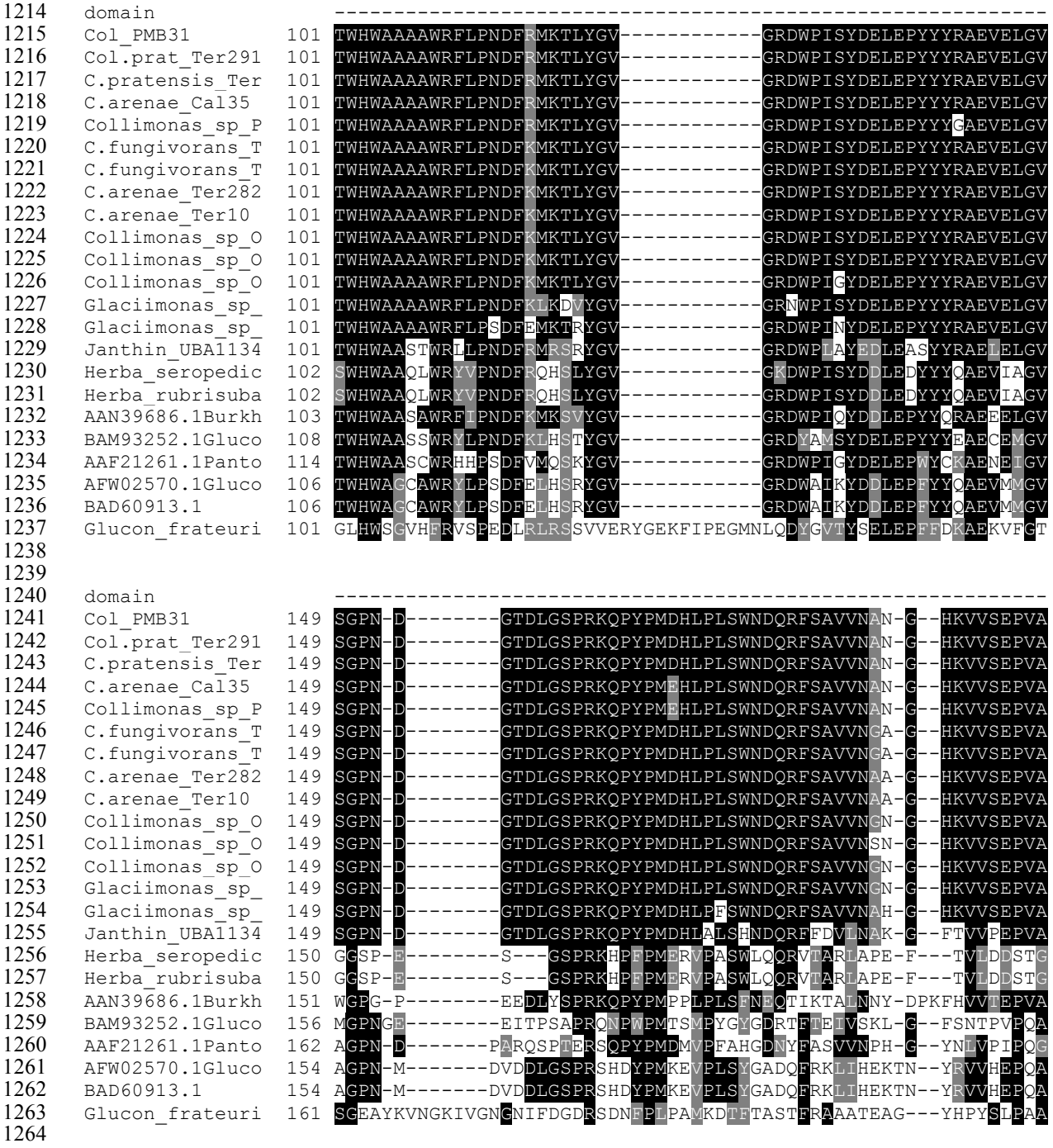
domain
Col_PMB31 101
Col.prat_Ter291 101
C.pratensis_Ter 101
C.arenae_Cal35 101
Collimonas_sp_P 101
C.fungivorans_T 101
C.fungivorans_T 101
C.arenae_Ter282 101
C.arenae_Ter10 101
Collimonas_sp_O 101
Collimonas_sp_O 101
Collimonas_sp_O 101
Glaciimonas_sp_ 101
Glaciimonas_sp_ 101
Janthin_UBA1134 101
Herba_seropedic 102
Herba_rubrisuba 102
AAN39686.1Burkh 103
BAM93252.1Gluco 108
AAF21261.1Panto 114
AFW02570.1Gluco 106
BAD60913.1 106
Glucon_frateuri 101
domain
Col_PMB31 149
Col.prat_Ter291 149
C.pratensis_Ter 149
C.arenae_Cal35 149
Collimonas_sp_P 149
C.fungivorans_T 149
C.fungivorans_T 149
C.arenae_Ter282 149
C.arenae_Ter10 149
Collimonas_sp_O 149
Collimonas_sp_O 149
Collimonas_sp_O 149
Glaciimonas_sp_ 149
Glaciimonas_sp_ 149
Janthin_UBA1134 149
Herba_seropedic 150
Herba_rubrisuba 150
AAN39686.1Burkh 151
BAM93252.1Gluco 156
AAF21261.1Panto 162
AFW02570.1Gluco 154
BAD60913.1 154
Glucon_frateuri 161

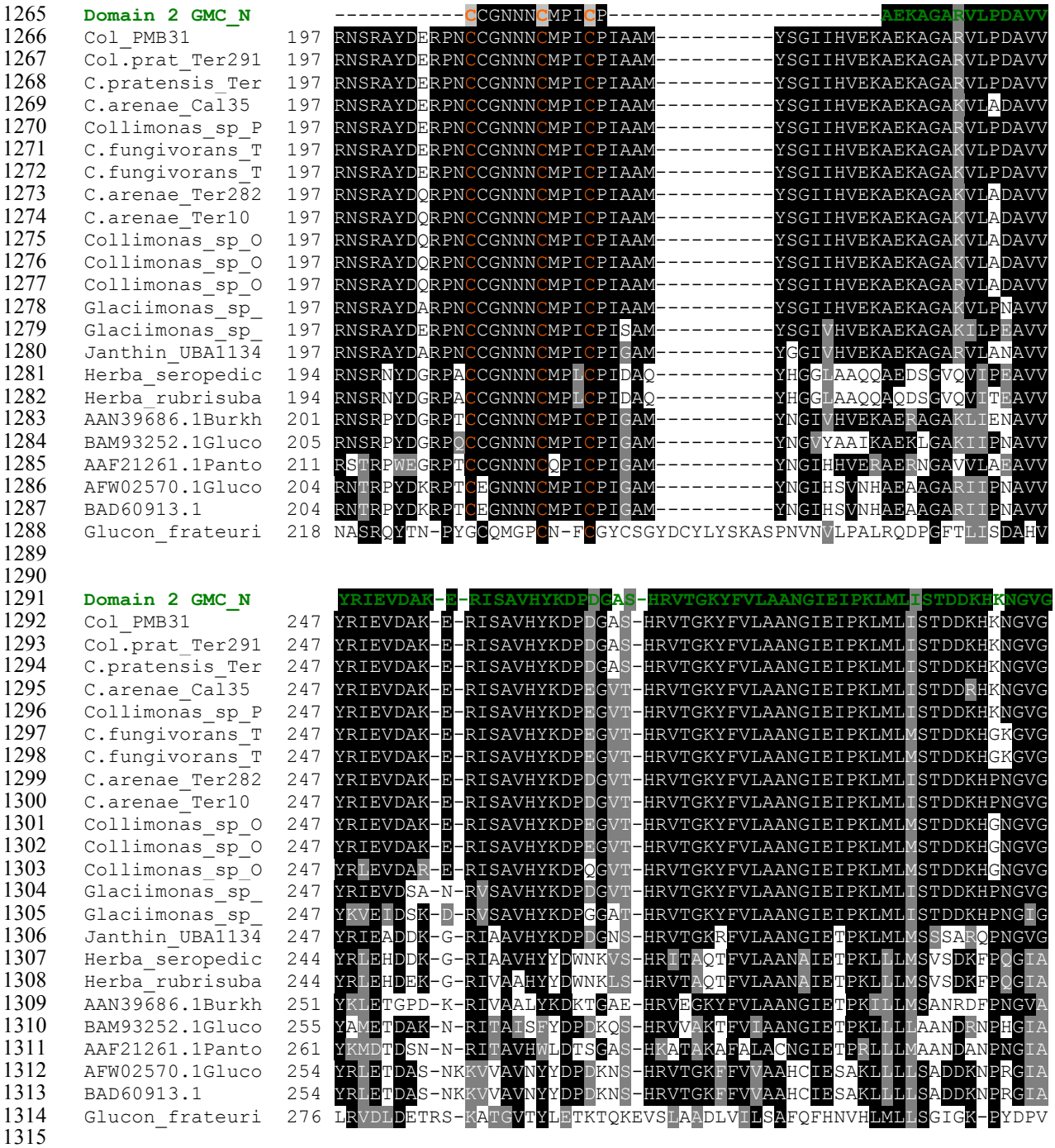
Domain 2 GMC_N
Col_PMB31
Col.prat_Ter291
C.pratensis_Ter
C.arenae_Cal35
Collimonas_sp_P
C.fungivorans_T
C.fungivorans_T
C.arenae_Ter282
C.arenae_Ter10
Collimonas_sp_O
Collimonas_sp_O
Collimonas_sp_O
Glaciimonas_sp_
Glaciimonas_sp_
Janthin_UBA1134
Herba_seropedic
Herba_rubrisuba
AAN39686.1Burkh
BAM93252.1Gluco
AAF21261.1Panto
AFW02570.1Gluco
BAD60913.1
Glucon_frateuri
Domain 2 GMC_N
Col_PMB31
Col.prat_Ter291
C.pratensis_Ter
C.arenae_Cal35
Collimonas_sp_P
C.fungivorans_T
C.fungivorans_T
C.arenae_Ter282
C.arenae_Ter10
Collimonas_sp_O
Collimonas_sp_O
Collimonas_sp_O
Glaciimonas_sp_
Glaciimonas_sp_
Janthin_UBA1134
Herba_seropedic
Herba_rubrisuba
AAN39686.1Burkh
BAM93252.1Gluco
AAF21261.1Panto
AFW02570.1Gluco
BAD60913.1
Glucon_frateuri

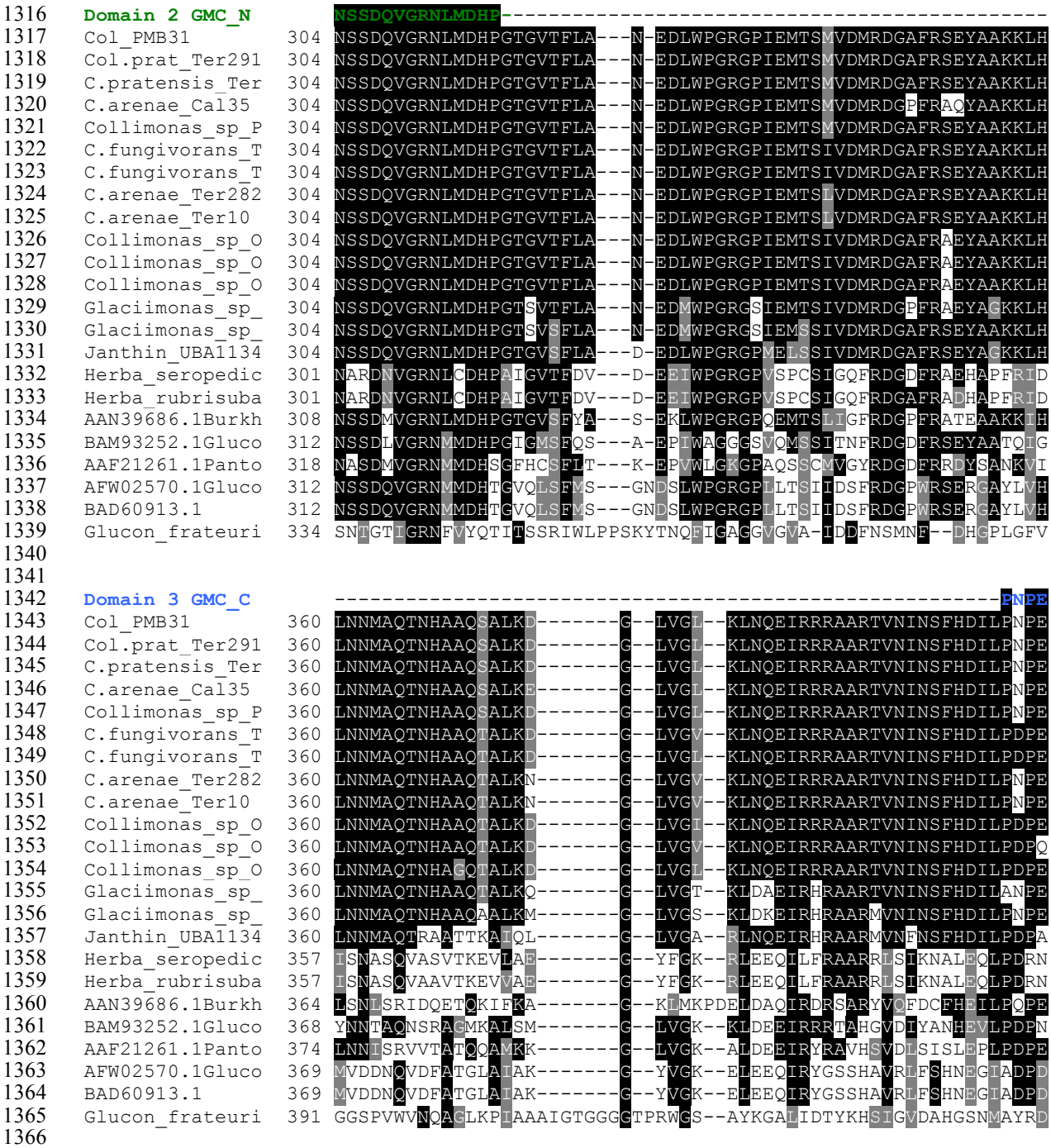
Domain 2 GMC_N
Domain 3 GMC_C
Col_PMB31
Col.prat_Ter291
C.pratensis_Ter
C.arenae_Cal35
Collimonas_sp_P
C.fungivorans_T
C.fungivorans_T
C.arenae_Ter282
C.arenae_Ter10
Collimonas_sp_O
Collimonas_sp_O
Collimonas_sp_O
Glaciimonas_sp_
Glaciimonas_sp_
Janthin_UBA1134
Herba_seropedic
Herba_rubrisuba
AAN39686.1Burkh
BAM93252.1Gluco
AAF21261.1Panto
AFW02570.1Gluco
BAD60913.1
Glucon_frateuri

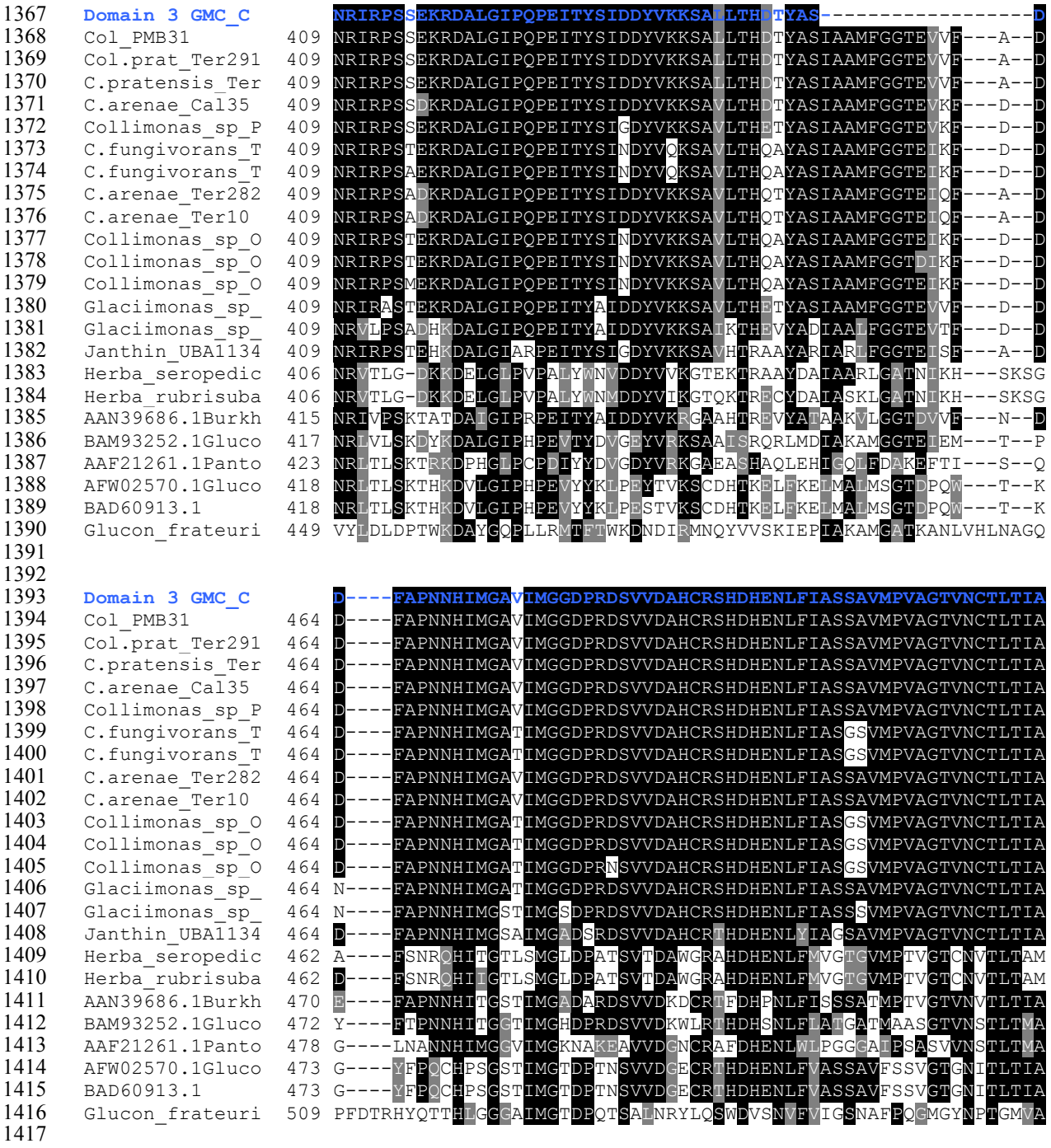
Domain 3 GMC_C
Col_PMB31
Col.prat_Ter291
C.pratensis_Ter
C.arenae_Cal35
Collimonas_sp_P
C.fungivorans_T
C.fungivorans_T
C.arenae_Ter282
C.arenae_Ter10
Collimonas_sp_O
Collimonas_sp_O
Collimonas_sp_O
Glaciimonas_sp_
Glaciimonas_sp_
Janthin_UBA1134
Herba_seropedic
Herba_rubrisuba
AAN39686.1Burkh
BAM93252.1Gluco
AAF21261.1Panto
AFW02570.1Gluco
BAD60913.1
Glucon_frateuri
Domain 3 GMC_C
Col_PMB31
Col.prat_Ter291
C.pratensis_Ter
C.arenae_Cal35
Collimonas_sp_P
C.fungivorans_T
C.fungivorans_T
C.arenae_Ter282
C.arenae_Ter10
Collimonas_sp_O
Collimonas_sp_O
Collimonas_sp_O
Glaciimonas_sp_
Glaciimonas_sp_
Janthin_UBA1134
Herba_seropedic
Herba_rubrisuba
AAN39686.1Burkh
BAM93252.1Gluco
AAF21261.1Panto
AFW02570.1Gluco
BAD60913.1
Glucon_frateuri

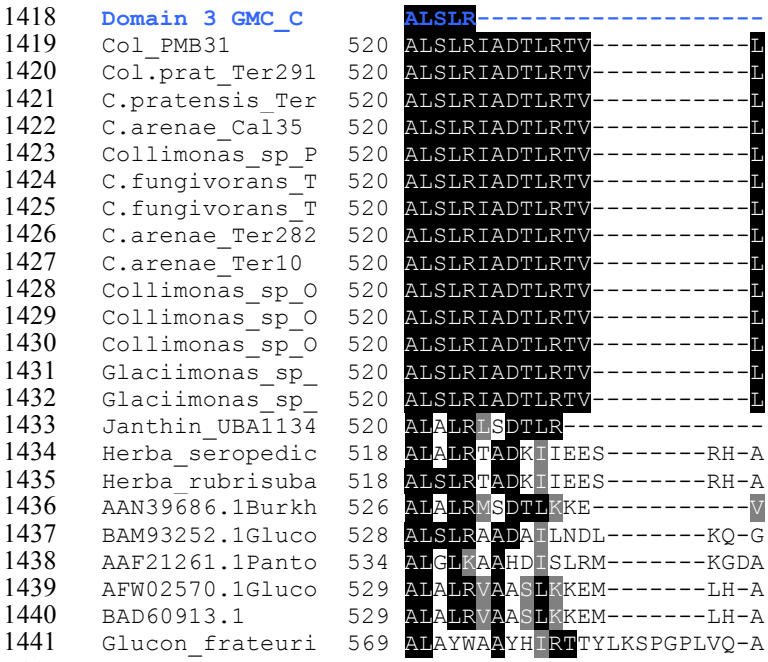

Figure S2: Highlight of the active domains detected in the large subunit of the GMC enzyme and of the cysteine rich region

Domain 1 : FAD ; Domain 2 and 3 correspond to GMC sites. Each line corresponds to a protein sequence and its localisation. The abbreviations correspond to those presented in the phylogenetic tree in Figure 6. Gluc_BAH805545.1, gluconate dehydrogenase; Gluc_BAD60913.1, sorbitol dehydrogenases; Burkholderia, glucose dehydrogenase; Gluc_japonicus, fructose dehydrogenase; Pantoea_agglo., choline dehydrogenase; Gluc_oxydans, sorbitol dehydrogenases.

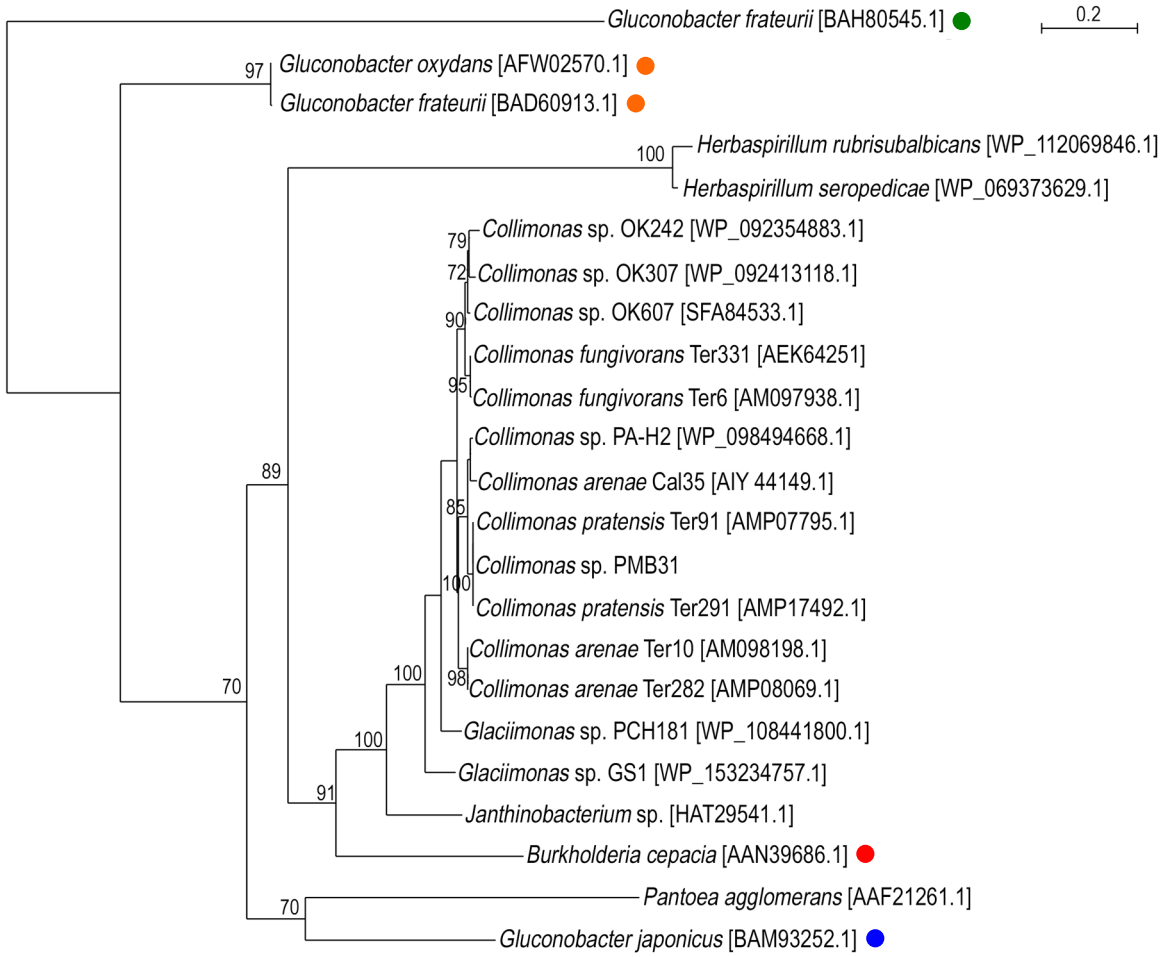

Figure S3: Phylogenetic tree based on protein sequence of the large subunit of different GMC-DH

Comparison of the GdhL sequence from PMB3(1) with homologous protein sequences from a set of 22 different genera or species related to *Collimonas* and available on international databases were analysed among them, 11 were assigned to the *Collimonas* genus. Other genera taxonomically close to *Collimonas* were chosen (*Glaciimonas*, *Janthinobacterium, Herbaspirillum* and *Burkholderia)*. Enzymes belonging to the GMC family and with a demonstrated function were included in the analysis such as Gluconate DH (GADH ; green circle), Sorbitol DH (SDH ; orange circle), Frcutose DH (FDH ; blue circle) and Glucose DH (GDH ; red circle). For these protein sequences, the accession number from NCBI is indicated between brackets.

1465

1466

1467

1468

1469

1470